RIGA TECHNICAL UNIVERSITY

Mārcis Priedītis

DEVELOPMENT AND RESEARCH OF POWER ELECTRONIC CONVERTERS FOR ADJUSTABLE TRANSFORMERS

Summary of the Doctoral Thesis

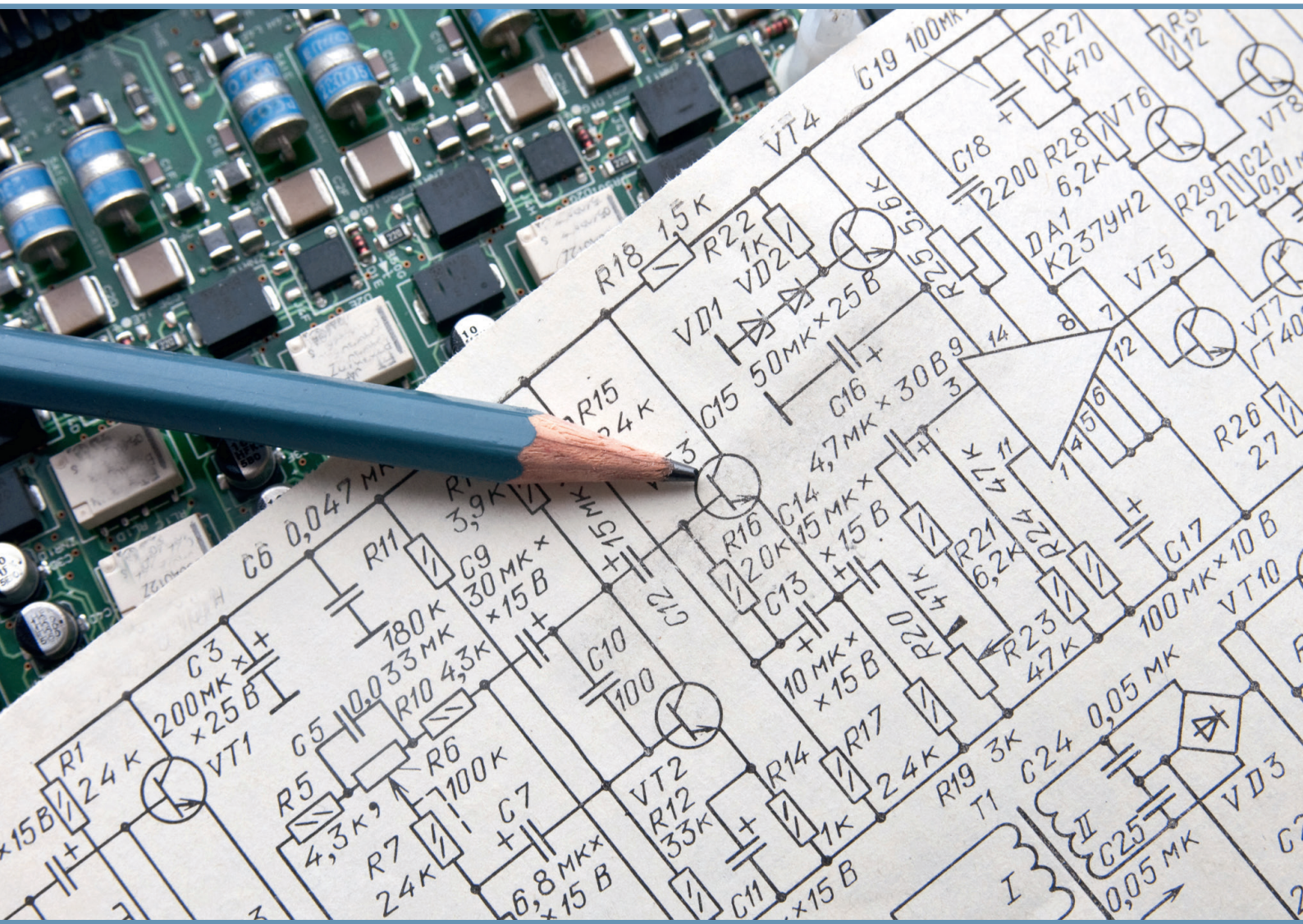

RTU Press
Riga 2021

RIGA TECHNICAL UNIVERSITY
Faculty of Electrical and Environmental Engineering
Institute of Industrial Electronics and Electrical Engineering

Mārcis Priedītis
Doctoral Student of the Study Programme "Computerized Control of Electrical Technologies"

DEVELOPMENT AND RESEARCH OF POWER ELECTRONIC CONVERTERS FOR ADJUSTABLE TRANSFORMERS

Summary of the Doctoral Thesis

Scientific supervisor
Professor Dr. habil. sc. ing.
IVARS RAŅĶIS

RTU Press
Riga 2021

Priedītis, M. Development and Research of Power Electronic Converters for Adjustable Transformers. Summary of the Doctoral Thesis. Riga: RTU Press, 2021. 56 p.

Published in accordance with the decision of the Promotion Council "RTU P-14" of January 18, 2021, Minutes No. 04030-9.12.2/1.

There is not all knowledge on Earth,

there is only constant overcoming of ignorance.

O. Vācietis

Sincere thanks for the support in the development of the dissertation to the scientific supervisor I. Raņķis, wife Baiba, for allowing our common time to be sacrificed and replaced by thought streams on electrical engineering topics, parents and grandparents for relentless external motivation to complete the dissertation and sending related materials for review and inspiration!

https://doi.org/10.7250/9789934226151
ISBN 978-9934-22-615-1 (pdf)

DOCTORAL THESIS PROPOSED TO RIGA TECHNICAL UNIVERSITY FOR THE PROMOTION TO THE SCIENTIFIC DEGREE OF DOCTOR OF SCIENCE

To be granted the scientific degree of Doctor of Science (Ph. D.), the present Doctoral Thesis has been submitted for the defence at the open meeting of RTU Promotion Council on 30 April 2021 at 13.00 online.

OFFICIAL REVIEWERS

Professor Dr. sc. ing. Jānis Zaķis
Riga Technical University, Latvia

Professor Dr. sc. ing. Elizaveta Liivik
Tallinn University of Technology, Estonia; Aalborg University, Denmark

Professor Dr. sc. ing. Voitech Stankevič
Vilnius Gediminas Technical University, Lithuania

DECLARATION OF ACADEMIC INTEGRITY

I hereby declare that the Doctoral Thesis submitted for the review to Riga Technical University for the promotion to the scientific degree of Doctor of Science (Ph. D.) is my own. I confirm that this Doctoral Thesis had not been submitted to any other university for the promotion to a scientific degree.

Mārcis Priedītis ……. (signature)

Date: ……

The Doctoral Thesis has been written in Latvian. It consists of Introduction; 4 chapters; Conclusions; 108 figures; 9 tables; the total number of pages is 109. The Bibliography contains 77 titles.

CONTENTS

GENERAL OVERVIEW

Actuality of topic

Transformer which can be used for addition or subtraction of voltage from source voltage is a well-known technical device. It is usually built on the basis of autotransformer [62]–[64] and has much less power rating than power rating of the load when working with low voltages on secondary winding [62]. In Russian technical literature such specific transformers are called adding transformers (*вотодабовочный трансформатор* [62]), but in the scientific literature of other countries it is called injection transformer [63], [64]. Taking into account positive properties of the device it is widely used in AC regulation in wide range of economic sectors, for example, for voltage stabilization in electric networks in countryside regions.

To make possible efficient use of such device, it has to be supported with automatic regulation solutions. In older solutions such regulation is done by switching between transformer secondary side windings by the help of mechanical, electromechanical, electromagnetic or simply unregulated electronic switches [62]. Regulation is neither wide enough and smooth, nor efficient.

Current development state of electronic technologies easily allows to use wide variety of electronic equipment for voltage regulation, mainly they are quite high frequency fully controllable semiconductor pulse regulators [65]. Most widely such systems are explored for DC circuits and systems where pulse regulation enables contactless and smooth regulation with very high efficiency indicators – efficiency close to 1, regulation amplitude from very small load and source voltage ratios (lower than 0.05) to tenfold ratios [65]. The first of this kind of DC regulators are called buck DC/DC regulators, the second – with higher output voltage than source voltage – boost DC/DC regulators [65]. To combine the regulation amplitudes of previously described regulators, buck/boost DC pulse regulators are used. Systems can be either unidirectional with one polarity regulated load voltages or bidirectional and with changeable output signal polarity [65].

At the same time, for AC circuits such regulators are rarely to be met in industrial applications. Such regulation, although can be found in scientific papers [3], [4], [25], is not even described in special technical literature on the topics of electrotechnics. At the same time, there exist technical problems which could be solved by the use of smooth contactless AC circuit regulators with high technical parameters [30]–[32]. Such devices could be used in lighting systems, electrotechnology systems, AC electric drive systems and others [11]–[13]. Nowadays, direct AC regulation is acquired by the use of one operation semiconductor devices (thyristors, simistors or triacs) which can be turned on at any time when current could flow in their conduction direction, but switching off happens only when current reaches zero value, which in AC systems is ensured at the moment of polarity change [65]. In such a way discrete switch regulation angle changes can be acquired, however constant in each half-period. Such systems are called AC regulators. Efficiency of such regulators usually is close to 1, however, the AC circuit current lag caused by the switch-controlled switching time time

lag causes a forced phase shift in the AC circuit between voltage and current, which determines a reduced power factor (*P* active power, *S* – total power) of regulated circuit.

In addition, circuits controlled in such a way cannot operate with sinusoidal load voltages, as a result part of total power *S* is understood as distortions power *T* [65], because of which ratio *P*/*S* is reduced even more; in addition, because of higher harmonics ratio between source currents, the 1st harmonic of and RMS source current is even more is reduced. That is indicated by THD which with this kind of regulation can exceed the recommended values.

Since phase regulated systems are widely used (because others are not in use today), compensation of high THD is one of the most important topics today, which in the end of the day is a parameter that affects efficiency of electronic systems. Higher order harmonics does not create positive real power but generates extra heat in wires and other passive components.

Taking into account the previously stated, it is clear that new methods should be explored in order to achieve more efficient AC regulation, and one of the solutions is pulse regulation with modern fully controlled semiconductor technologies. In such a way, it would be possible to reach wider regulation amplitude, to ensure smoother regulation with low values of THD, low power factor and high efficiency. In addition, introduction of such systems allows to increase the range of applications [7], [9], [34], [35].

The main difficulties that have so far limited the introduction of AC pulse control systems are as follows.

1. Industrially usable fully controllable AC transistors are still not developed (although they are being studied [21], [22]) and therefore the switching mechanism must be combined in different ways (reverse-parallel, series-connected and reversible bridge elements to ensure bidirectional control). Taking into account the influence of the inductive elements of the AC circuits, it is necessary to create additional circuits for the dissipation of electromagnetic energy, which requires an increased number of switches as well as thinking about the right switching moments of switches [20], [56].
2. AC circuits have more controllable parameters than DC circuits (amplitude, RMS value, phase shift, frequency, THD and *P*/*S* value, etc.), which expands and complicates the development of real systems.
3. AC systems mostly are more powerful than DC systems which require more complex technical solutions. It is also important to overcome the prevailing view in the technical community that simple thyristor/triac regulators are quite sufficient in AC circuits.

In view of the above, it is clear that there is a need to intensify research into the development of improved control systems for AC systems. The simplest way to solve the problems of regulating AC systems is to involve DC stages in the AC system and perform various regulating and transforming actions in them, because they are developed and well researched [33]. However, it is not possible to regulate all AC electrical parameters in DC stages [28], as well as by implementing DC stages, sales costs increase sharply and the system efficiency decreases.

Therefore, the use of DC stages is not an effective solution. Looking at different AC objects, it can be seen that in the vast majority of them various coordinating elements are introduced, basically different transformers. Electronic regulation of these parameters could also affect the regulation of the whole system. Therefore, many scientists are developing an AC control system and reducing research to the development of transformer – typical electromagnetic converter – pulse control systems [14]–[16], [63], [64]. In addition, taking into account the characteristics of injection-type transformers, which are related to the effect of partial circuit control on the control parameters of the whole system, it is clear that extensive attention is paid to these objects and their control in the overall AC systems [10], [14], [18], [19].

Looking at the sources of information on electronic control systems for injection transformers, it can be seen that currently the main focus is on high-speed compensation of short-term voltage drops and swell surges in the low-voltage network [39], [42], [49], [50]. Such systems are designed in different ways, both by connecting control circuits on the low voltage side of the transformer and on the high voltage side [45], [66], as well as by making combined circuits. The most comprehensive study of such systems has been presented [5] by a group of scientists led by Jacek Kaniewski, University of Zielona Gora, Poland. Other studies can be found here in [24], [26], [27], and [59].

Research has also been carried out in AC control systems without injection transformers, and equipment that can perform the intended task has been developed, but the semiconductor elements used must be able to withstand higher currents and voltages than when voltage regulator circuits include transformers. The dimensions of AC regulators without transformers are smaller than the dimensions of regulators with them [36]–[38], [40], [43], [44], [58].

However, despite the fact that serious research has been conducted and published in the study of electronic regulators of injection transformer systems, it cannot be said that everything in this field has been studied. Basically, all the considered and known works lack fundamental research of electromagnetic processes in electronic control systems themselves, very little research has been done on the AC quality filters of regulated AC circuits and the choice of their parameters, and the range of technical applications is quite limited.

In view of all the above, it can be stated that the development of modern electronic power regulation principles and equipment for AC objects, circuits and systems is a very topical technical and scientific task which requires both new and effective principles of such systems and research and calculation methods on the basis of which mathematical descriptions of various AC voltage regulation systems are created in order to study their properties and to define the objects, branches and directions of application.

Objectives and Main Tasks

The aim of this work is to expand and deepen the knowledge base on the theoretical and practical aspects of operation of electronic transformer control systems for injection transformers and AC circuits and systems. The tasks include extending the development of different variants of unipolar and bipolar voltage regulation of primary and secondary

winding voltages by high-frequency pulse regulators and researching their applications, using both new theoretical methods and experimenting with different system models and summarizing their possible characteristics so that they can be more widely and more effectively used in practical applications.

Scope of the Work and Research Objects

The scope of the work includes various injection transformer systems for regulation of effective values of load voltage and phase shifts between input and load voltages, as well as mathematical descriptions of their operation, research of properties, and creation of characteristics. Various known and newly developed regulatory schemes and regulatory management principles are the objects of work.

Scientific Novelty of the Work

Substantiated method of calculation of AC voltage pulse control systems based on fundamental harmonic use of modulated voltages and currents both in analytical calculations and process research on the basis of vector diagrams in which fundamental harmonic signals are presented in vector form.

Several AC pulse control schemes have been developed for various load voltage and phase adjustment systems at both single-phase and three-phase power supplies. A standard scheme of modulated voltage sinusoidal filtering has been developed, the parameters of such a scheme and their dependence on mutual changes of parameters based on the application of regression statistical methods have been studied.

Practical Significance of the Work

All created new schemes and methods are practically applicable in practice and provide an opportunity to obtain new technical effects. The practical application for the dissertation is an extensive mathematical description of processes and relationships in different control schemes depending on the size of the load and other influence factors.

Methods and Tools Used

The main research method is based on the in-depth mathematical research of electromagnetic processes using basic equations of electrical engineering and research methods of AC circuits, verification of results and calculations are mainly done by computer modelling methods in PSIM and MatLab. All mathematical calculations are aimed at the fundamental harmonic expression of modulated signals and the evaluation of the effect on inductive electrical circuits.

Theses to be Defended

1. Modulation processes must be divided into two standard groups – with unipolar and bipolar generation of modulation results; the results of the first are defined in 1/0 categories, where 1 state in the case of AC corresponds to its instantaneous value in the active part of the modulation period, but bipolar – is defined in –1/+ 1 categories, where +1 in each modulation period corresponds to the instantaneous value of AC directly, but –1 corresponds to the reverse polarity.
2. The influence of modulated voltage or current on other system elements is determined by their fundamental harmonic waves and their basic characteristics – amplitudes and RMS values, which in turn depend on the main operating characteristics of the modulation switching element – switching frequency and relative active duration in the switching period (factor *D*).
3. Fundamental harmonic waves in circuit vector diagrams can be characterized by appropriately scaled vectors with defined lengths and shift angles. The fundamental harmonic parameters of modulated signals can be determined by the Fourier transform method for analogue signals.
4. It usually makes sense to create a modulation effect with a constant factor *D* in one modulated AC period, modulation against one load can be performed from both single-phase and multi-phase AC, and the position of the modulation switch active state interval during the modulation period determines the type of modulation effect.

Scientific Publications of the Author

1. Raņķis, I., Priedītis, M., Staņa, Ģ. Investigation of Direct AC-AC BUCK Converter with Series Injection Transformer. In: 2018 IEEE 59th International Scientific Conference on Power and Electrical Engineering of Riga Technical University (RTUCON 2018): Conference Proceedings, Latvia, Riga, 12–14 November 2018. Piscataway: IEEE, 2018, pp. 1–5. ISBN 978-1-5386-6904-4.
2. Raņķis, I., Priedītis, M. Properties of the AC/AC Buck-Boost Converter. In: 2017 IEEE 58th International Scientific Conference on Power and Electrical Engineering of Riga Technical University (RTUCON 2017), Latvia, Riga, 12–13 October 2017. Piscataway: IEEE, 2017, pp. 188–193. ISBN 978-1-5386-3847-7.
3. Priedītis, M., Raņķis, I. Necessity of Low Range Voltage Stabilization and solution with Transformer Based AC Pulse Modulation System. In: Advances in Information, Electronic and Electrical Engineering (AIEEE 2015): Proceedings of the 2015 IEEE 3rd Workshop, Latvia, Riga, 13 November 2015. Piscataway: IEEE, 2015, pp. 111.-114. ISBN 978-1-5090-1202-2.
4. Raņķis, I., Priedītis, M., Širkins, D. Transformer Based AC Pulse Modulation System for Voltage Stabilization. In: 2015 IEEE 5th International Conference on Power Engineering, Energy and Electrical Drives (POWERENG): Proceedings, Latvia, Riga, 11–13 May 2015. Riga: RTU Press, 2015, pp. 600–605. ISBN 978-1-4673-7203-9.

5. Raņķis, I., Priedītis, M. Buck Mode Control Methods of the qZS-Resonant DC/DC Converters. In: 19th European Conference on Power Electronics and Applications, Poland, Warsaw, 11–14 September 2017. Warsaw: 2017, pp. 1–16.
6. Ivars Raņķis, Mārcis Priedītis, Aigars Vītols. Investigation of the Effectiveness of Nonlinear Inductor in the AC/DC Node of Three Phase Rectifier. The 7th IEEE Workshop on Advances in Information, Electronic and Electrical Engineering (AIEEE'2019), 2019.

Conference Reports

1. 7th IEEE Workshop on Advances in Information, Electronic and Electrical Engineering (AIEEE'2019).
2. 18th International Symposium "TOPICAL PROBLEMS IN THE FIELD OF ELECTRICAL AND POWER ENGINEERING" and "Doctoral School of Energy and Geotechnology III".
3. 20th European Conference on Power Electronics and Applications (EPE'18 ECCE Europe).
4. IEEE 59th International Scientific Conference on Power and Electrical Engineering of Riga Technical University (RTUCON 2018).
5. 19th European Conference on Power Electronics and Applications; (EPE'17 ECCE Europe).
6. IEEE 58th International Scientific Conference on Power and Electrical Engineering of Riga Technical University (RTUCON 2017).
7. 16th International Symposium "TOPICAL PROBLEMS IN THE FIELD OF ELECTRICAL AND POWER ENGINEERING" and "Doctoral School of Energy and Geotechnology III".
8. 5th IEEE Workshop on Advances in Information, Electronic and Electrical Engineering (AIEEE 2015).
9. 15th International Symposium "TOPICAL PROBLEMS IN THE FIELD OF ELECTRICAL AND POWER ENGINEERING" and "Doctoral School of Energy and Geotechnology III".
10. IEEE 5th International Conference on Power Engineering, Energy and Electrical Drives (POWERENG 2015).

1. INVESTIGATION OF INJECTION TRANSFORMER PARAMETERS IN VOLTAGE REGULATION SYSTEMS

Although injection transformers (IT) are well-known objects of electrical systems, their descriptions in the known literature sources do not pay enough attention to the peculiarities of regulation in all modes of operation. Therefore, in order to facilitate a common understanding of the types and characteristics of operations an overview and study of the IT parameters and characteristics of regulation has been carried out here.

1.1. Injection Transformer Circuit Diagrams and Their Properties

The autotransformer system can be considered as a type of series injection transformer, where the supply voltage U_1 is connected to the transformer primary winding w_1 but the secondary winding w_2 with a lower voltage and number of turns, and the common point can be connected with the primary winding in series (matched or opposite directions) in the load circuit (Fig. 1.1). The main relations can be determined by considering the two windings to be perfectly magnetically connected, regardless of the other parameters of the transformer replacement circuit. In this case, the relation between winding voltages and currents is determined only by factor $K = w_2/w_1$, it is the ratio of the number of secondary and primary turns of both windings. Both the rated power of the IT against the rated power of the load and the range of changes in the load voltage depend on this factor.

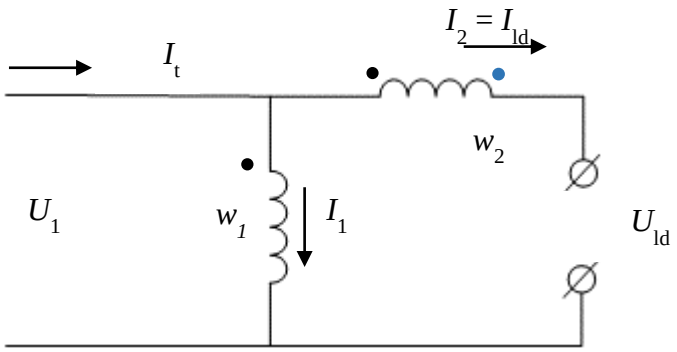

Fig. 1.1. Series injection transformer with opposite winding connection (excluding the blue dot) / matched winding connection (including the blue dot).

The vector diagrams corresponding to both connections – opposite-connection and matched – are shown in Fig. 1.2. In the case of an opposite winding connection (down-reducing), the primary winding current, which is part *K* of the load current, is opposite to load current, and as a result less current is consumed from the source than the load current.

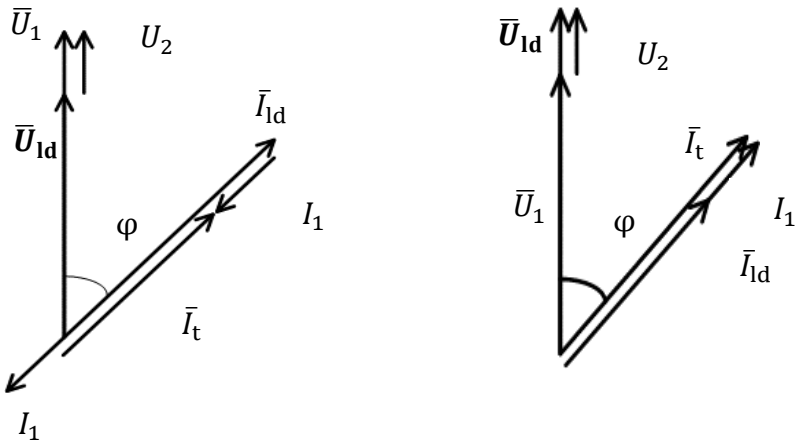

a) b)

Fig. 1.2. Simplified vector diagrams of injection transformer a) with oppositely connected windings and b) with matched direction winding connection.

In a matched connection of IT windings (up circuit), the current in the primary winding coincides in phase with the load current, and as a result the current consumed from the source is greater than the load.

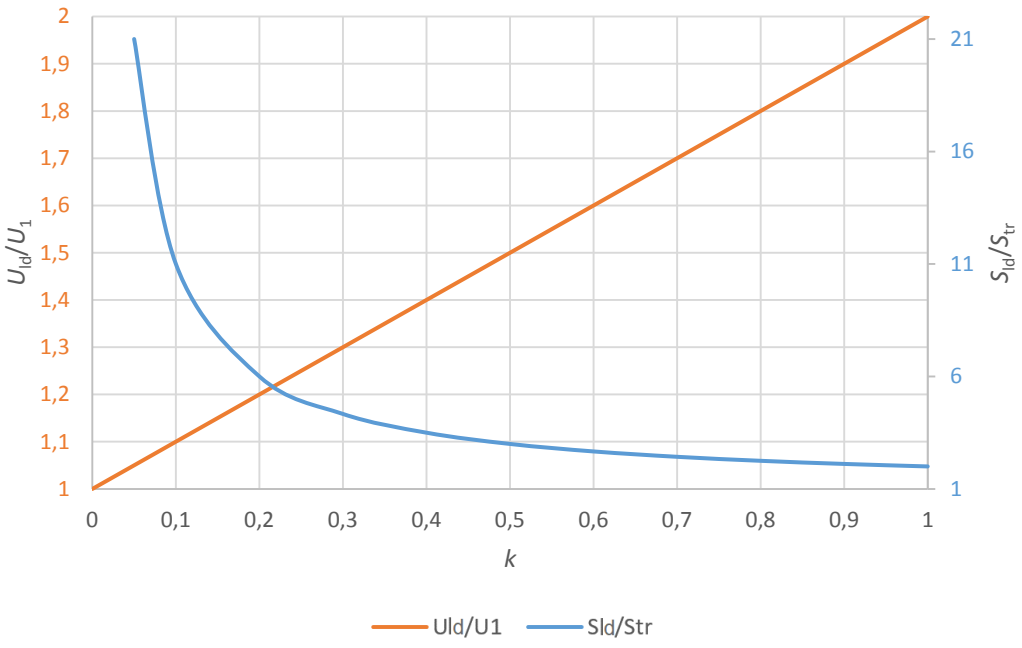

Fig. 1.3. Diagrams characterizing an IT circuit with matched winding connection.

The rated power of the injection transformer is the nominal voltage of the secondary winding multiplied by the rated current of the load, and since $U_2 = KU_1$ and K is less than 1 (usually only 0.05…0.25 in compensation tasks) but the load voltage is $U_{ld} = U_1(1 + K)$ or $U_1(1 – K)$, respectively, then the power of the transformer is about K times less than the load, which is also the main basis for the efficiency of IT application. In Fig. 1.3 it is shown how

the load voltage and transformer power in the matched circuit depend on the assumed K. As can be seen, if K = 0.1, then the load voltage is 10 % higher than the source voltage, but the transformer power is about 10 % of the load power.

Since the primary winding current of the transformer is the Kth part of the load current, it is clear that at low K it is advantageous to perform control actions in the primary winding circuit, even though its voltage is high. On the other hand, although the secondary winding has a high current, the voltage is low, which also actually determines that the regulation can be carried out efficiently in the secondary winding circuit.

1.2. Influence of Real Parameters of Injection Transformer on System Relations

In order to take into account a real injection transformer (IT) model in calculations and research, it is necessary to create a specific IT sample with a defined capacity, to calculate the parameters of its replacement scheme and implement them in the obtained calculation systems. However, it is also possible to estimate the parameters of the substitution scheme. For example, to determine the winding resistances from the actual losses in the transformer windings, which can be roughly determined by the efficiency factor, assuming that all losses are only electrical. The resistance of the primary winding is then determined from the relationship

$$I_1^2 R_1 + \frac{I_1^2}{K^2} R_1 K^2 = I_{\mathrm{ldN}} K U_1 (1 - \eta), \tag{1.1}$$

where η is the efficiency factor which can be assumed to be 0.95 in approximate calculations. The resistance of the primary winding is then calculated as

$$R_1 = \frac{0.05\, U_1}{2 K I_{\mathrm{ldN}}} = \frac{0.025 U_1^2}{S_{\mathrm{trN}}}, \tag{1.2}$$

where I_{ldN} is the rated load current, and S_{trN} is the rated power of the transformer.

For example, if K = 0.1, U_1 = 230 V, and I_{ldN} = 5 A, i.e. the rated power of the transformer is around 115 VA, then the resistance of the primary winding should be taken as 11.5 Ω. The resistance of the secondary winding reduced to the primary winding will be the same.

In turn, the inductances of windings can be roughly determined from the calculations of the short-circuit experiment, assuming the ratio of short-circuit voltage (impedance voltage) U_K* = 0.09 (this value is recommended for approximate calculations). Then

$$L_1 + L_2 = \frac{0.09 K U_1}{2\pi f I_{\mathrm{ldN}}} = \frac{0.09 K^2 U_1^2}{2\pi f S_{\mathrm{trN}}} \tag{1.3}$$

Considering that $L_1 = L_2/K^2$, the inductance of the primary winding is $(1 + K^2)$ times less than the sum, but the inductance of the secondary winding reduced to the primary winding will be as high as L_1. For example, if K = 0.1, U_1 = 230 V, f = 50 Hz, and I_{ldN} = 5 A, then the inductance of the primary winding is L_1 = 1.32 mH.

The inductance of the magnetizing circuit can be determined from the no-load experiment: the no-load current, which is about 0.1 of the nominal of the transformer, passes through the magnetizing inductance and is therefore determined as

$$L_{\mathrm{m}} = \frac{U_1}{0.1 I_{\mathrm{ldN}} 2\pi f K}. \tag{1.4}$$

For example, if $K = 0.1$, and $I_{\mathrm{ldN}} = 5$ A, then $L_{\mathrm{m}} = 14.7$ H.

To test the influence of the assumed transformer parameters on the modelling results, computer modelling was performed with $K = 0.1$, different transformer winding parameters and in all 3 cases (*R* load, *RL* load, 1f bridge rectifier TG, assuming the effective value of the load current at 5 A. Studies have shown that the largest errors occur at inaccurately set magnetization inductance values in the models (Table 1.1).

Table 1.1

Computer Modelling Results at Different Transformer Winding Resistances and Leakage Inductances

Circuit load type; transf. parameters	Magnetization inductance	Load current rms, A	Source current rms, A	Primary winding current rms, A	Power factor, *P*/*S*	Current THD
Resistive (transf. *R*, *L* calculated)	14.7 H	5.02	4.52	0.509	$PF_1 = 0.989$ $PF_2 = 1$	0
Resistive (trans. *R*, *L* 100× smaller)	14.7 H	5.04	4.55	0.12	$PF_1 = 0.989$ $PF_2 = 1$	0
RL load (trans. *R*, *L* calc.)	14.7 H	5.01	4.54	0.489	$PF_2 = 0.928$ $PF_1 = 0.925$	0
RL load (tr. *R*, *L* 100× smaller)	14.7 H	5.02	4.55	0.487	$PF_2 = 0.927$ $PF_1 = 0.925$	0
TG with *RL* load (trans. *R*, *L* calc.)	14.7 H	5.04	4.55	0.488	$PF_1 = 0.957$ $PF_2 = 0.959$	$THD_2 = 0.1884$ $THD_1 = 0.188$
TG with *RL* load (100× smaller transf. *R*, *L*)	14.7 H	5.05	4.56	0.487	$PF_1 = 0.958$ $PF_2 = 0.94$	$THD_2 = 0.1883$ $THD_1 = 0.189$

As can be seen, if the magnetizing inductance of a transformer of appropriate size is set, which is calculated to be 14.7 H, then changes in transformer winding resistance and leakage inductance in the range of 100 times below the calculated values practically do not affect the main calculation results – the current values and consumed and realized power and its quality parameters – current THD (Total Harmonics Distortion indicator) and power factors *PF*.

In in-depth study of current THD and the *P*/*S* factor (power factor) of the power consumed from the source, it can be observed that the THD depending on the parameters in both IT systems (down and up connections) is below 0.3, which is a relatively good indicator (Fig. 1.4), and this parameter is better at lower L_m.

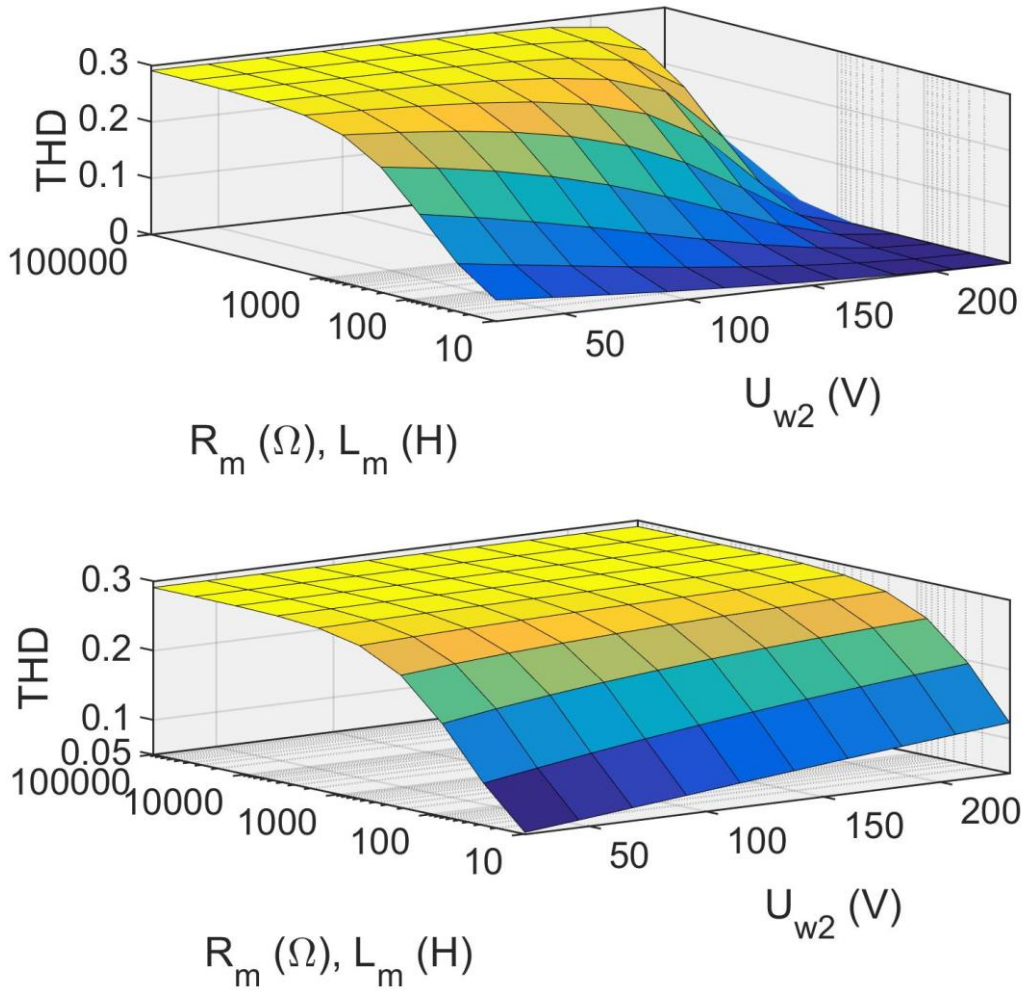

Fig. 1.4. Dependence of the source current THD on the transforming conductive inductance L_m and the loss resistance R_m of this circuit in the case of a single-phase bridge rectifier load with *R*, *L* load at its output; top chart for down option, bottom chart – up option.

In-depth research shows that setting the inductance of magnetization plays an important role in assessing the quality of power consumed and sent to load. Fig. 1.4 shows the obtained diagrams of current THD dependence on the inductance of the magnetizing circuit and the equivalent resistance R_m of its magnetic loss. It turns out that at a constant *K*, the higher L_m and R_m, the worse the THD. The diagrams were obtained for mass computer modelling with various parameters.

Conclusions of Chapter 1

1. The value of the current flowing in the IT secondary winding is the same as the load current, but the current in the primary winding depends on the set winding ratio factor $K = w_2/w_1 < 1$. The lower it is, the lower the power consumption in the primary winding and the associated control circuit, which allows the primary winding circuit to be used efficiently for the electronic control of the load power. However, with a lower transformation factor K, the influence of the control circuit on the load voltage is also smaller, i.e., the load voltage control range is reduced.
2. The rated power of the injection transformer is determined by the voltage of the secondary winding and the product of the load current, and if $K < 1$, then this power is less than the full power of load S_{ld}. The lower the K, the lower the rated power of the transformer is almost K times, but the relative range of the load voltage regulation, which is $2K$, decreases. The AC power S consumed from the power supply and sold at the load are the same, the quality indicators of these powers – the power factor P/S and the harmonic distortion factor THD – are practically the same for both powers.
3. As the research of computer models shows, the main importance of the adequacy of the model is the correct setting of the IT magnetic inductance, if it is set too low, then the transformative link is weakened; variations in other parameters are not too important.

2. DISCRETE AND MODULATED VOLTAGE CONTROL OF INJECTION TRANSFORMERS IN THE PRIMARY WINDING CIRCUIT WITH FACTOR *D* FIXED ELECTRONIC SWITCH DURING THE VOLTAGE PERIOD

In traditional systems, it is customary to implement transformer winding switching with mechanical or electromechanical switches, thus performing discrete load voltage regulation. The regulation is not fluid, the operating modes of the contact switches are difficult, the quality of the regulation is poor. The voltage regulation scheme with switching of the transformer secondary winding outputs, which allows to implement discrete voltage regulation at the system output, is shown in Fig. 2.1.

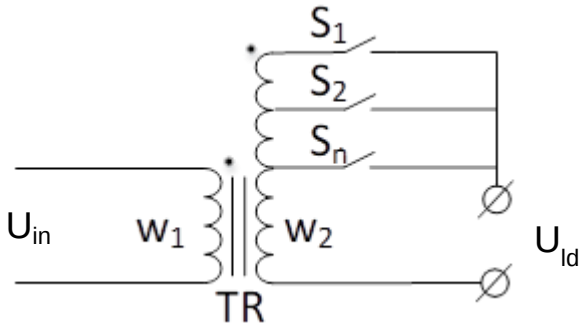

Fig. 2.1. Transformer discrete voltage regulation scheme.

Circuits that regulate the voltage level in this way are described in several articles [15]–[18]. They are usually intended to replace conventional electromechanical voltage regulators due to their slow operation and sparking (at switching times). Thyristors or simistors (triacs) are usually used as switches due to their current and voltage resistance. The circuits have been studied with the intention of using them to set the voltage level at low voltage distribution points [16], [17] or at medium voltage distribution points [15].

Input and output voltages are related:

$$U_{\mathrm{ld}} = K_n U_{\mathrm{in}}. \tag{2.1}$$

2.1. Calculations in Circuits with Sinusoidal and AC Switch Modulated Voltage and Current Signals

The term “vector diagram” refers to sinusoidal signals. In cases where these signals are modulated, vector diagrams cannot be drawn to represent the variable signals under consideration in a fixed coordinate system. However, if a method is used that is based on using the RMS value of the modulated signal to generate a new sinusoidal unmodulated signal (which is a fundamental harmonic signal), then this new signal can be represented in a vector diagram. See Fig. 2.2.

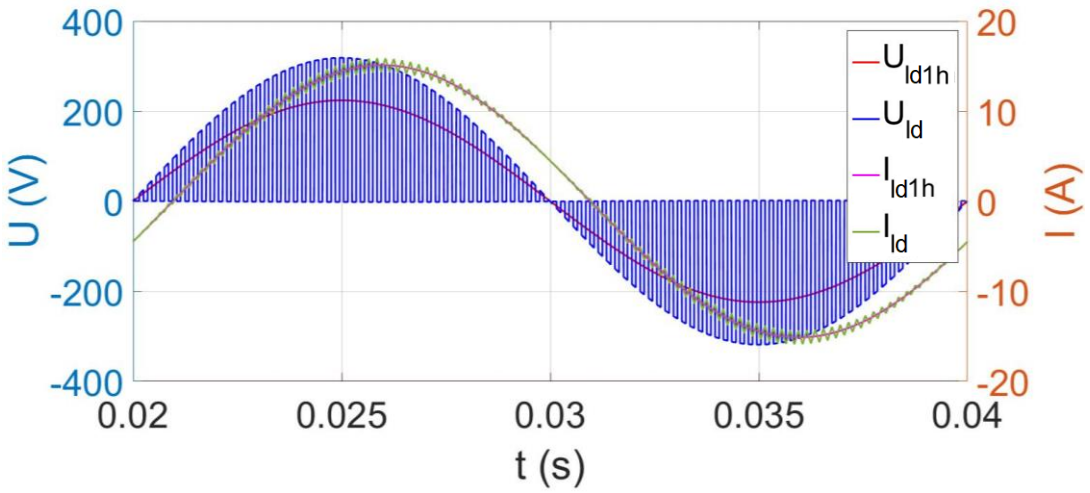

Fig. 2.2. Replacement of modulated signals with sinusoidal signals. jI_{ld} and jU_{ld} are the current and voltage signals used in the vector diagrams (base-harmonic of modulated signals). Here the amplitude of the modulated voltage is 320 V, f = 50 Hz, D = 0.5, R = 10 Ω, L = 10 mH.

The basic harmonic curve of the modulated voltage is composed of the average values of the voltage in each successive modulation interval – this means that for the modulated curve shown in Fig. 2.2 with D = 0.5 in each modulation period, the fundamental harmonic curve equals $u_{(1)} = Du = DU_m \sin\omega t$, where U_m is the amplitude value of the source voltage (modulated) and $\omega = 2\pi f$, and f is the frequency of this voltage (in our studies f = 50Hz).

This modulated voltage basic harmonic in a modulated voltage-fed resistive inductive circuit generates a practically sinusoidal current with corresponding instantaneous current strokes during the voltage pulse and pause (during pause in the direction of zero, during pulse – in the direction of voltage pulse peak – positive and negative). The fundamental harmonic amplitude and RMS value of this current are $I_{(1)m} = DU_m/Z$, respectively, but the RMS value $I_{(1)} = DU_m/((\sqrt{2}Z)$, where Z is the impedance of the RL circuit. If the circuit time constant is 3–5 times the modulation period or $L/R = (3\ldots5)\cdot(1/f_m)$, where f_m is the modulation frequency (usually several kHz), then the instantaneous current strokes are negligible against the fundamental harmonic of the current and may be disregarded. In Fig. 2.2 the RMS value of the load current (measured with an ammeter) is I_{ld} = 10.8 A, Z = 10.48 Ω, the RMS value of the fundamental harmonic of the modulated voltage is $U_{(1)ef}$ = 113.18 V, but the calculated amplitude of this basic harmonic is 160 V, thus fully compliant with the assumption described.

This example proves that it is justified to obtain the basic harmonic of the modulated AC voltage by using the method of sequential composition of the AC voltage period from the average voltage values in modulation intervals. On the other hand, since direct measurement of the fundamental harmonic of the modulated voltage with measuring instruments is not possible, because it is in a sense Mean Wave, indirect measurement can be used with *RL* target with defined *Z* connection to the modulated voltage, measured current is the RMS value of the fundamental harmonic. As already mentioned, the circuit time constant must be 3…5 times greater than the modulation period.

2.2. Operation of AC Switches in IT Primary Windings

2.2.1. Modulator Buck Operation with Control of *D* of Primary Winding

If the IT primary winding is regulated so that it is periodically connected to the source and then disconnected (Fig. 2.3) while resetting it, then we consider that it is **unipolar** regulated by changing the connection fill factor *D*. The *D* factor is the ratio of the switch's active state interval in the switching period to this period. Here, **unipolar** means that the winding voltage does not change polarity during the switching period – in the positive period of the input voltage it is positive polarity and zero, in the negative period it is negative polarity and zero.

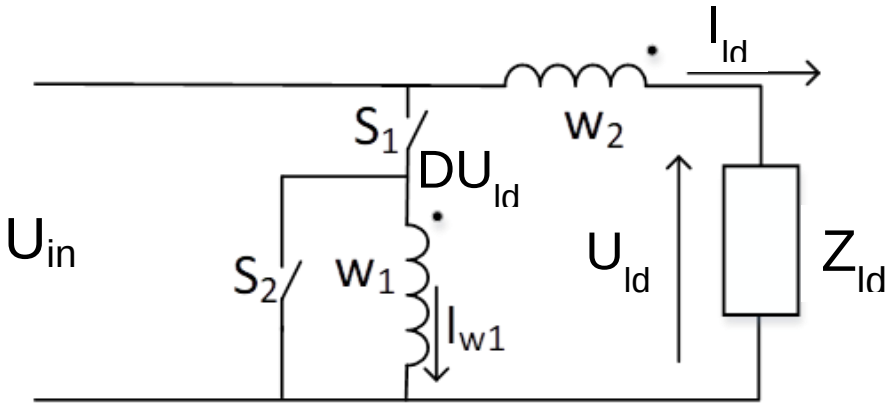

Fig. 2.3. Unipolar load voltage regulation with IT and constant filling factor *D*.

In such a circuit, switches S_1 and S_2 operated alternately, generating a "meander" shaped signal at the output (Fig. 2.4), if the load is not only active then the current signal is, of course, in phase offset from the voltage signal. U_{in} = 230 V, $w_2/w_1 = K$ = 0.1, R_{ld} = 10 Ω, L_{ld} = 5 mH. The modulation frequency of 500 Hz is chosen low for better signal shape display. The modulation frequency of such circuits usually exceeds several kHz.

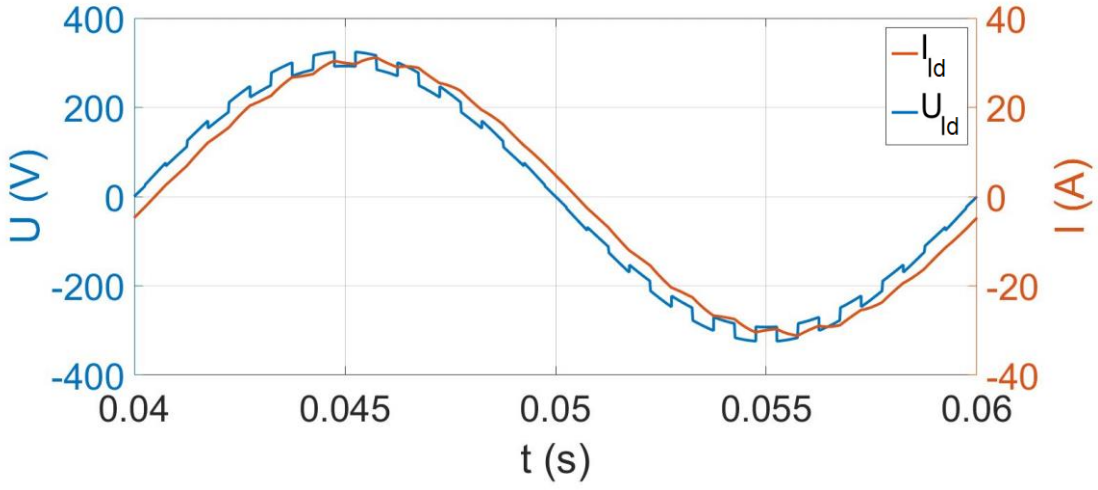

Fig. 2.4. Voltage and current curves for active inductive loads.

In unipolar modulation, the fundamental harmonic curve of the voltage of the primary winding IT is formed as DU_1, and this curve transmits through the transformer windings to the load circuit, where the voltage depends on the product of transformers K and D. In the winding matching case circuit shown in Fig. 2.3, the load voltage is formed as

$$U_{\text{ld}} = U_1(1 + KD) \tag{2.2}$$

but, if a winding opposite connection is used, then

$$U_{\text{ld}} = U_1(1 - KD). \tag{2.3}$$

For example, if K = 0.1 and U_1 = 230 V, then in a matched circuit, the voltage can be changed smoothly with a change of D from 230 V at D = 0 to 253 V at D = 1. In turn, when winding opposite connection in IT is used, then voltage is reduced to 207 V.

At D = 0.5 with K = 0.1 and U_1 = 225 V in a coordinated connection under load with R = 50 Ω, L = 10 mH the effective value of voltage was 237.2 V, and the effective current with a practically completely sinusoidal current curve 4.75 A (calculated at 4.73 A). The THD value of the measured load voltage curve at f_{m} = 5 kHz was 0.1. Load voltage and current modulation by IT and modulation effects are shown in Fig. 2.5.

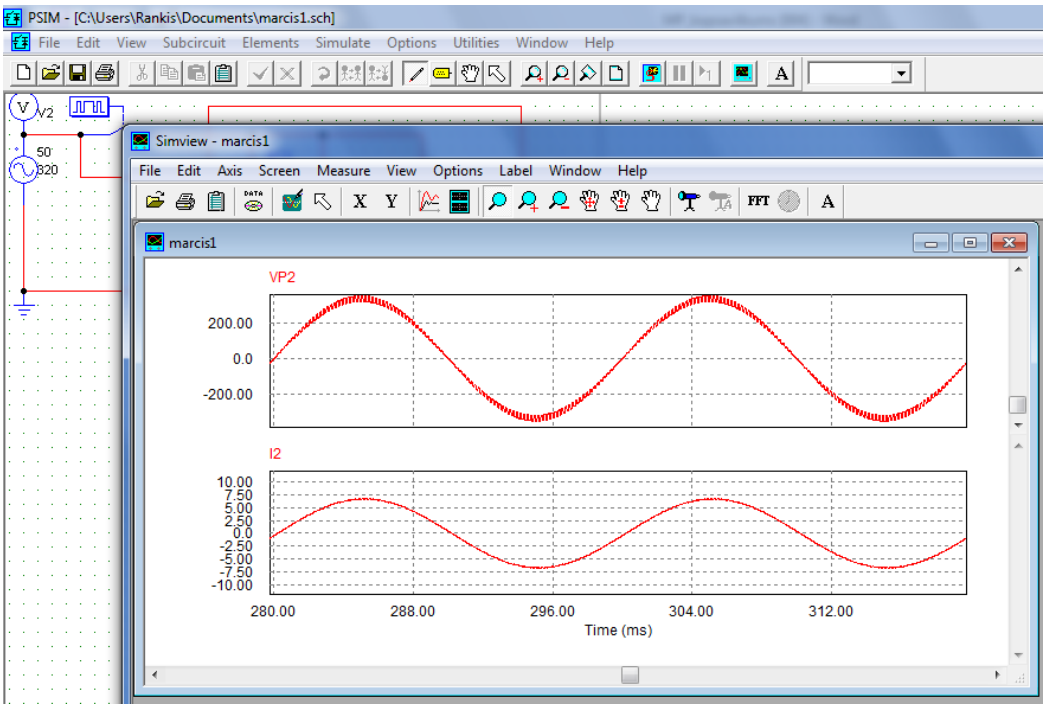

Fig. 2.5. Load voltage and current modulation by IT and modulation effects.

2.3. Modulator Buck Operation with Direct Primary Winding PWM Control

2.3.1. Bipolar Modulation in AC Circuits

When ST is on (D interval), then $U_{\text{ld}} = U_1$, when SR is on (1 – D interval), then $U_{\text{ld}} = -U_1$ (Fig. 2.6). If during the half-period D is constant and thus also 1 – D, then 2 basic harmonics generated by each switch are formed, which form the base-harmonic of the load voltage.

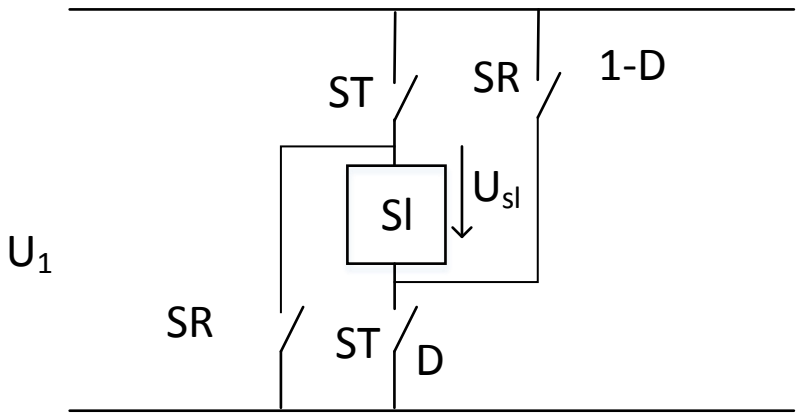

Fig. 2.6. Implementation scheme of bipolar modulation principle.

The *D* interval (direct connection) produces a base-harmonic direct wave

$$u_{\mathrm{ld}D} = DU_{1\mathrm{m}}\sin\omega t. \tag{2.4}$$

In turn, in the (1 – *D*) interval (reverse connection) a reverse wave is formed

$$u_{\mathrm{ld}(1-D)} = -(1-D)U_{1\mathrm{m}}\sin\omega t. \tag{2.5}$$

In general, the resulting basic harmonic is formed on the load:

$$\begin{aligned} u_{\mathrm{ld}(1)} = u_{\mathrm{ld}D} + u_{\mathrm{ld}(1-D)} &= U_{1\mathrm{m}}\sin\omega t(D-1+D) \\ &= (2D-1)U_{1\mathrm{m}}\sin\omega t. \end{aligned} \tag{2.6}$$

If $D > 0.5$, then the phase between $U_{\mathrm{ld}(1)}$ and U_1 is zero because the direct connection is longer in the modulation period, but when $D < 0.5$, this phase is 180° because the reverse connection is longer. By changing *D* in relation to the value $D = 0.5$, the load voltage can be both in phase and in opposite phase with U_1. If $U_{\mathrm{ld}(1)}$ is used as the input voltage in another system, then this property provides the reversibility of the input signal.

Starting from the changes in *D*, the given control curve is obtained – the RMS value of the base-harmonic of the load voltage as a function of *D* (Fig. 2.7).

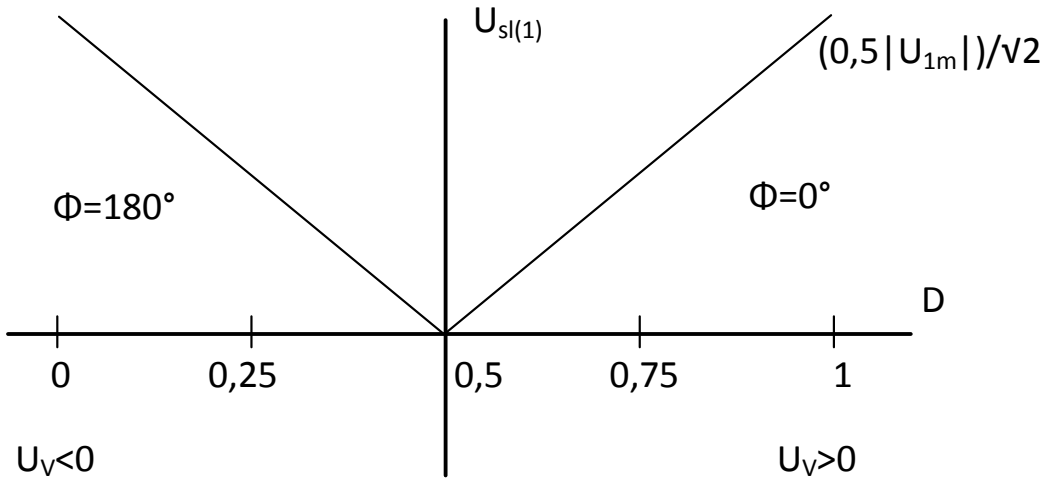

Fig. 2.7. Load voltage and phase versus source voltage control curve.

If, for example, the IT primary winding w_1 is used as the load, which is connected to the secondary winding w_2 with the coefficient $K = w_2/w_1$, and both windings are connected in matched directions, then at $D < 0.5$ the real secondary winding operates in the opposite phase and IT load voltage reduction occurs:

$$U_{\text{ldIT}} = U_1 + U_1 K(2D - 1), \tag{2.7}$$

but at $D > 0.5$, the load voltage increases above the RMS value of the source voltage.

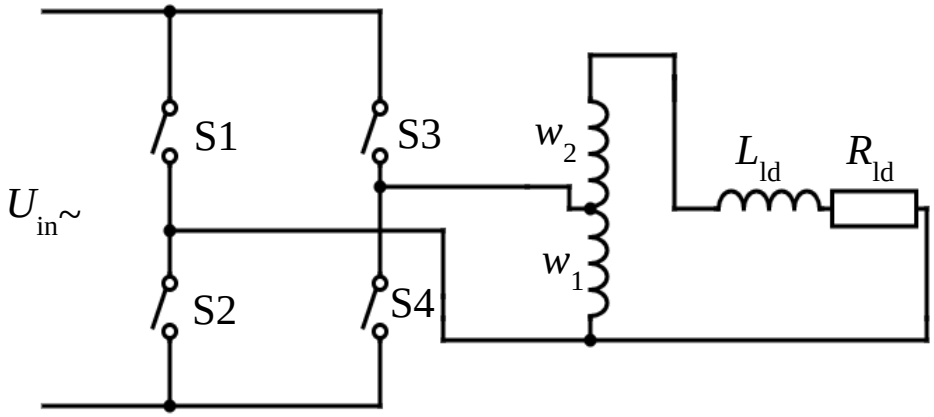

Fig. 2.8. Bipolar modulation circuit with IT up connection.

The switching ratio D can be changed by comparing the bipolar saw tooth voltage with frequency f_m with the DC control voltage U_v (Fig. 2.9).

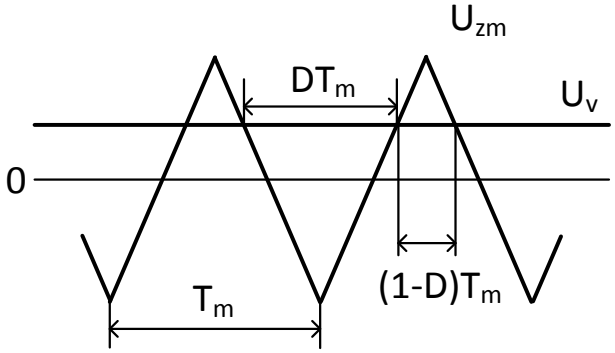

Fig. 2.9. Obtaining D by comparing saw tooth voltage with direct voltage.

The saw tooth voltage frequency f_m is many times higher than the source U_1 voltage frequency $f_m >> f_1$. It is usually taken in several kilohertz.

When $U_v > U_z$, control signals are generated on the direct connection switches ST, when $U_v < U_z$, then on the reverse connection SR switches. The relative duration of the direct connection interval in the modulation period $T_m = 1/f_m$ is

$$D = 0.5\left(1 + \frac{U_v}{U_{zm}}\right), \tag{2.8}$$

but reverse connection

$$1 - D = 0.5\left(1 - \frac{U_v}{U_{zm}}\right), \tag{2.9}$$

where U_{zm} is the amplitude of the saw tooth voltage. Usually U_{zm} is 10–20 V and if, for example, U_{zm} = 10 V, then U_r can be changed between –10 V and + 10 V. When U_v = 0 V, D = 0.5 and the fundamental harmonic RMS value of the modulator load is 0.

To test the principle, a computer model of such a system with U_1 = 230 V, k = 0.1, U_{zm} = 10 V, f_m = 5 kHz has been developed.

Depending on the control voltage, the following basic harmonic values of the IT load voltage were obtained (Table 2.1).

Table 2.1

Power Circuit Parameters Depending on the Set Control Signal

U_v	+5	–5	–10	+10
D	0.75	0.25	0	1
U_1	162.6	162.6	162	162.6
$U_{ld(1)}$	169.1	153.0	146.4	178.9
calc. $U_{ld(1)}$	170.7	154.6	146.1	179.9

As can be seen, bipolar modulation has provided control reversibility without changing the circuit, which is a great advantage of the system – regardless of the interconnection of IT windings the load voltage can be regulated both up and down from the source voltage level.

It can also be concluded that the simple calculation formulas give a very good agreement with the experimentally determined values.

However, this control method produces higher voltage ripple on the load than the method discussed above. Therefore, if pulsation-free load voltage is required, larger filters should be used than usual.

The dependence of the load voltage THD on the IT output voltage and the filling factor D is shown in Fig. 2.10. As can be seen, THD is very good, but increases with decreasing D (especially at higher K).

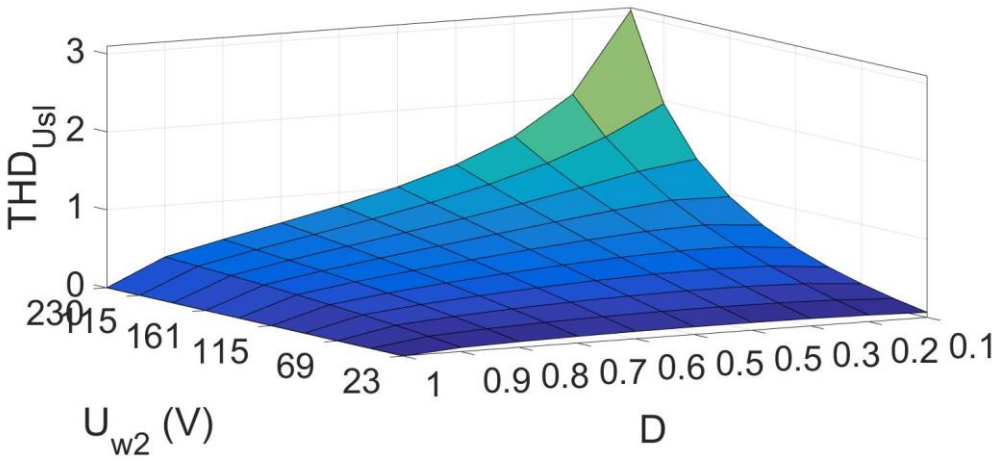

Fig. 2.10. Dependence of the load voltage THD on the RMS value of the IT secondary winding voltage and factor D.

2.4. Methods for Detecting Instantaneous Voltage Step-Wise Disturbances

Methods for detecting voltage disturbances have been extensively studied. Methods for determining voltage dips have been described in [52]–[54]. The most popular methods are as follows.

1. Maximum value recording method. This method is based on the search of the supply voltage wave gradient d*u*/d*t* and the amplitude or maximum value. When the wave gradient is zero, a comparison is made with a predetermined value. The control system can be set, for example, to signal a fault that deviates from the set-point by 5 %.

$$\text{Gradient} = \frac{U_t - U_{t-\Delta T}}{\Delta T}, \tag{2.10}$$

where U_t is the voltage value at time t and $U_{t-\Delta T}$ is the voltage value at time $t - \Delta T$. This method returns the magnitude of the fault, its start time and end time.

The disadvantage of this method is that it may be necessary to wait up to half of the cycle until information on the magnitude of the voltage fault becomes available, and signal noise may provide false information about the fault. This method does not provide information on the change of the phase shift angle at the moment of voltage disturbance.

2. Method of determining the average RMS value (every-period). This method is based on the determination of the average RMS value of the mains voltage and comparison with the preset value.

The average RMS value of the mains voltage can be determined using the following equation:

$$U_{\text{rms}} = \sqrt{\frac{1}{N}\sum_{j=1}^{N} u^2[j]}, \tag{2.11}$$

where N is the number of points at which the instantaneous value readings are taken in one cycle, and $u[j]$ is the value of the jth read voltage. The larger N, the more accurately U_{rms} can be determined.

The disadvantage of this method is that there is a one-cycle time delay in obtaining information on voltage disturbances, and low-order harmonic disturbances will cause calculation inaccuracies.

3. Method of determining the phase shift angle. This method is based on measuring the instantaneous value of the voltage several times in succession during each quarter period (throughout the period) and comparing it with the set values (Fig. 2.11).

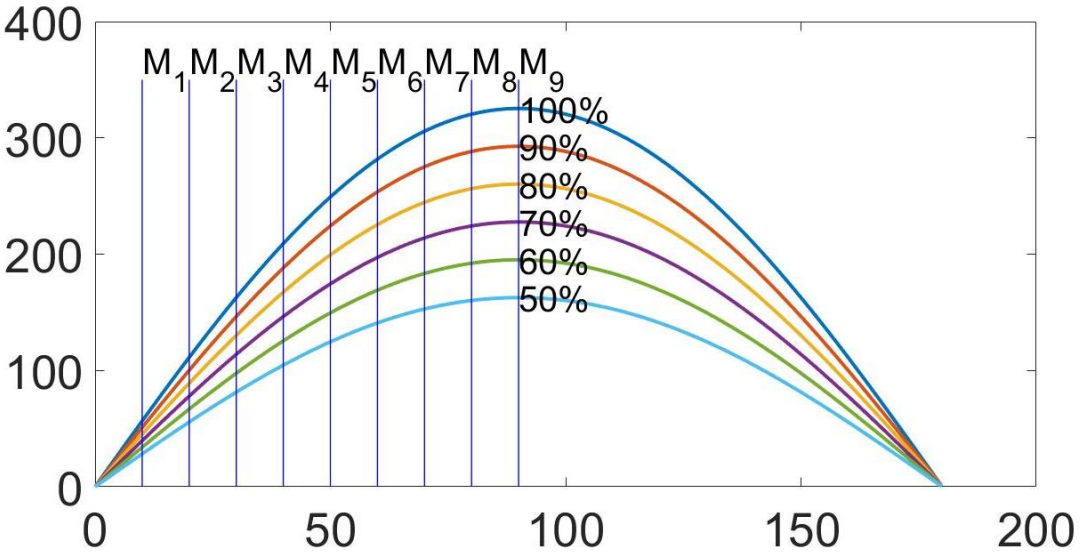

Fig. 2.11. Phase shift methods with sequential measurement of the instantaneous value of voltage and comparison with the set values.

This method is considered to be one of the fastest methods for detecting voltage disturbances. The more often the voltage is measured, the faster the change in voltage wave can be detected.

4. Method for determining the average effective voltage value (continuous). This method is based on the continuous comparison of a voltage wave with a "perfect" voltage wave. Interference from the input voltage is filtered out and a phase shift of 90° is performed. Then, as shown in Fig. 2.12, the obtained voltage signal is processed with the help of Pythagorean theorem and the length of the voltage vector is obtained (Fig. 2.12).

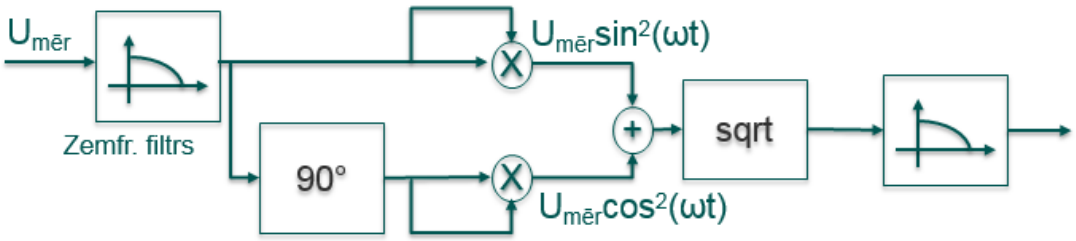

Fig. 2.12. Scheme for determining the value of the average effective voltage.

This method introduces a much lower latency assessment compared to that described in point 2.

5. Fall detection method developed in Riga Technical University [77]. It is a method by which voltage sags can be detected very quickly because the input signal is shifted in phase several times at relatively small angles and the amplitudes of these shifted signals are compared with each other. As a result, with small voltage changes, the phase-shifted voltages differ and the voltage change can be recorded. The phase shift is performed by means of the so-called multi-phase sensor, shown in Fig. 2.13.

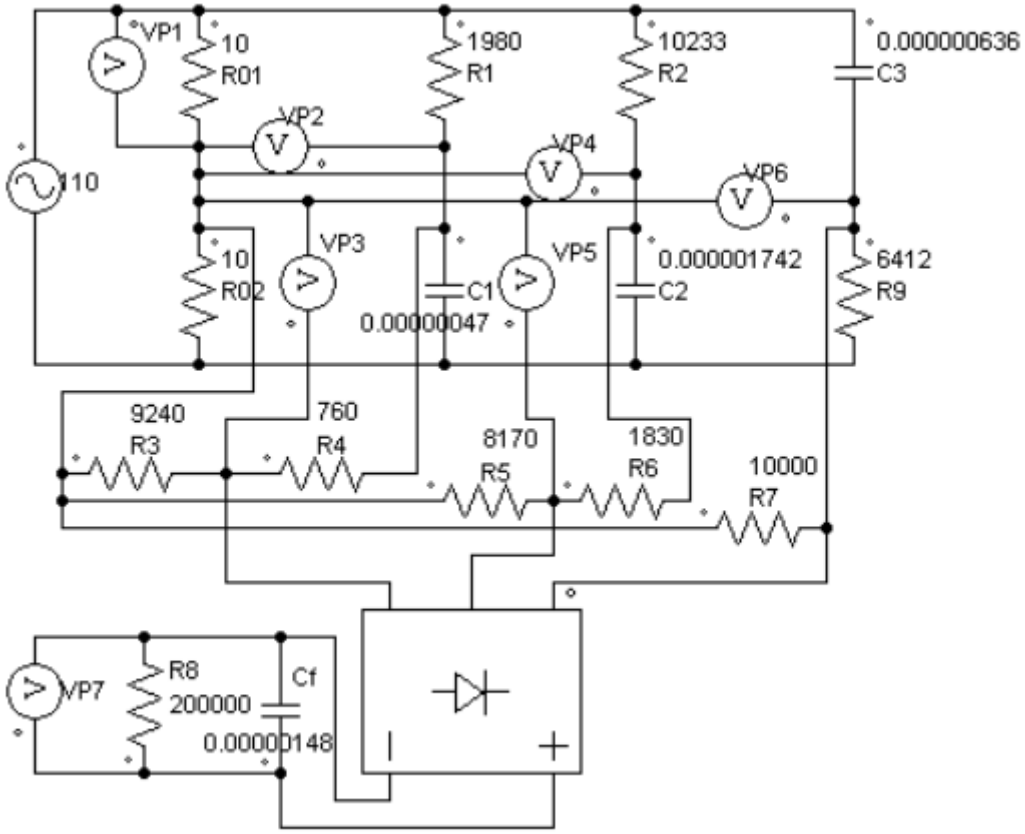

Fig. 2.13. Multi-phase sensor.

Conclusions of Chapter 2

1. If the modulation is performed with conditionally 2 switches, one of which connects the winding voltage and the other resets the winding in the case of an open winding, then conditional unipolar *D* modulation is performed, which forms a *D*-proportional proportional factor *D* and source voltage effective value multiplication.
2. As the modulated current is small against the load and source current, the effect on the latter's harmonic quality (THD indicator) is negligible.
3. The harmonic quality of the primary winding and, consequently, the secondary IT winding voltage can be improved by introducing an *LC* filter in the modulated primary winding circuit.
4. The introduction of additional reactive elements raises the issue of calculation methods for modulated AC circuits. The paper shows that as a result of 0/1 modulation of the source AC voltage, the fundamental harmonic of the voltage connected to the filter circuit determines the sinusoidal values of the current in the inductive circuits, but the modulation of sinusoidal circuits determines the sinusoidal voltage waveform parameters in the associated capacitive stages.
5. Using the mentioned approach, a vector diagram for a complex circuit was created on the basis of which the main parameters of such a circuit – voltage values on the load

capacitor, inductor current effective values, shift angles between different voltages and currents, etc. – were calculated.

6. The results obtained from the expressions coincide very well with those obtained in the practical models, which proves the validity of the approach.
7. The value of the filter voltage is sensitive to an increase in the load on the circuit connected to the capacitor, but as the statistical processing of the calculations for a sufficiently wide range of element parameters shows, this decrease can be compensated by a decrease in choke inductance with an increase in load.

3. ADVANCED SOLUTIONS FOR PULSE CONTROL OF INJECTION TRANSFORMERS

3.1. Effectiveness of AC/AC Buck–Boost Pulse Regulator Implementation in the Primary Winding Circuit

A lot of scientific articles have suggested the use of DC/DC solutions in AC converter circuits. Some authors suggest the use of traditional buck–boost circuits, which in the DC/DC version give the opposite voltage polarity at the output [23] but are increasingly based on converters that allow to obtain the same signal polarity at the output as at the input [23]–[25]. Usually, the principle of operation is described in scientific articles, simplified equations are used to describe the voltage gain, and the results of simulations and experiments are displayed. The purpose of this section is to give an insight into the relationships of the scheme shown in Fig. 3.1.

3.1.1. Principles and Operation of AC/AC Buck–Boost

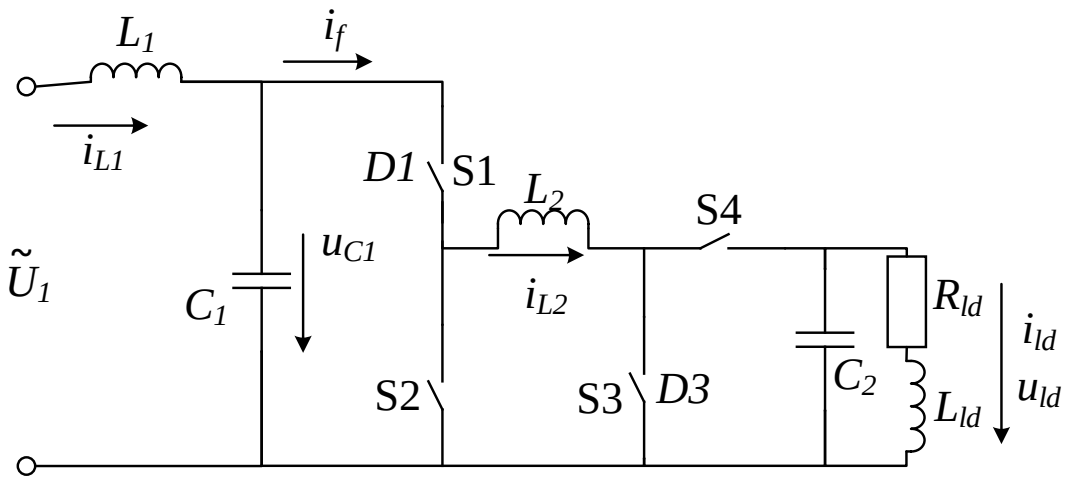

Fig. 3.1. Single-phase two-way AC/AC converter.

For the circuit to work, 4 bidirectional semiconductor switches S1, S2, S3, S4 must be used. While switch S4 is on and S3 is off, switches S2 and S1 operate the circuit in buck mode. While switch S1 is on and S2 is off, switches S3 and S4 operate the circuit in boost mode. Filters are used at both input and output of the circuit to ensure the required quality of voltage and current signals.

3.1.2. AC/AC buck–boost Pulse Controller Characteristics and Relationships

Assuming that the voltage (consisting of a series of closed resistors and inductors) and current are sinusoidal and shifted from each other by angle $\varphi_{ld} = \text{arctg}(\omega L_{ld}/R_{ld})$, where L and R are the load parameters but $\omega = 2\pi f$, vector diagrams (Fig. 3.2).

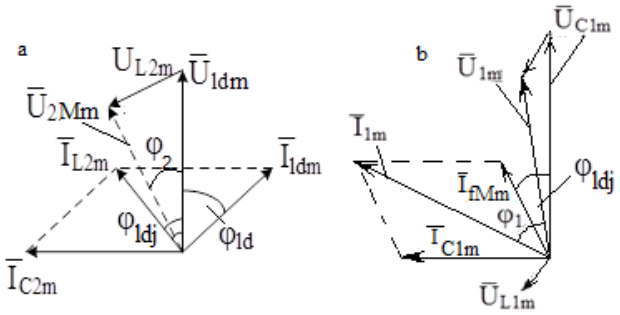

Fig. 3.2. Vector diagrams for a) load part and b) input filter part.

Using vector diagrams for buck and boost operation variants, it is possible to obtain mathematical relations (Table 3.1).

Table 3.1

Obtained Correlations for Buck and Boost Action Variants

Buck action option		**Boost action option**	
$I_{\mathrm{L2m}} = I_{\mathrm{ldm}}\sqrt{a}$	(3.1)	$i_{\mathrm{S4MB}} = (1 - D_3)i_{\mathrm{L2B}}$	(3.18)
$\varphi_{\mathrm{ldj}} = \mathrm{arctg}\dfrac{\omega(C_2 Z_{\mathrm{ld}}^2 - L_{\mathrm{ld}})}{R_{\mathrm{ld}}}$	(3.2)	$I_{\mathrm{S4MmB}} = I_{\mathrm{ldmB}}\sqrt{a}$	(3.19)
$i_{\mathrm{fM}} = D_1 I_{\mathrm{L2m}} \sin\left(v + \varphi_{\mathrm{ld}} + \varphi_{\mathrm{ldj}}\right)$	(3.3)	$I_{\mathrm{L2mB}} = I_{\mathrm{fmB}} = \dfrac{I_{\mathrm{ldmB}}\sqrt{a}}{1 - D_3}$	(3.20)
$u_{2\mathrm{M}} = u_{\mathrm{C1}} D_1$	(3.4)	$U_{\mathrm{S3MmB}} = (1 - D_3)U_{\mathrm{ldmB}}$	(3.21)
$U_{2\mathrm{Mm}} = I_{\mathrm{ldm}}\sqrt{Z_{\mathrm{ld}}^2 - 2Z_{\mathrm{ld}}\omega L_2\sqrt{a}\sin\varphi_{\mathrm{ldj}} + a\omega^2 L_2^2}$ $= \dfrac{U_{\mathrm{ldm}} b}{Z_{\mathrm{ld}}}$	(3.5)	$\bar{U}_{\mathrm{C1m}} = \bar{U}_{\mathrm{S3MmB}} + \bar{I}_{\mathrm{L2mB}}\omega L_2$	(3.22)
$U_{\mathrm{ldm}} = \dfrac{Z_{\mathrm{ld}} D_1 U_{\mathrm{C1m}}}{b} \cong \dfrac{z_{\mathrm{ld}}}{b} D_1 U_{1\mathrm{m}}$	(3.6)	$U_{\mathrm{C1m}}^2 = \left(U_{\mathrm{S3MmB}} - U_{\mathrm{L2mB}}\sin\varphi_{\mathrm{ldj}}\right)^2 + U_{\mathrm{L2mB}}^2\cos^2\varphi_{\mathrm{ldj}}$	(3.23)
$\tan\varphi_2 = \dfrac{U_{\mathrm{L2m}}\cos\varphi_{\mathrm{ldj}}}{U_{\mathrm{ldm}} - U_{\mathrm{L2m}}\sin\varphi_{\mathrm{ldj}}}$	(3.7)	$U_{\mathrm{ldmB}} = \dfrac{Z_{\mathrm{ld}} U_{\mathrm{C1m}}}{b(1 - D_3)}.$	(3.24)
$\varphi_1 = \mathrm{arctg}\dfrac{U_{1\mathrm{m}}\omega C_1 + D_1 I_{\mathrm{L2m}}\sin\varphi_{\mathrm{ldj}}}{D_1^2 I_{\mathrm{L2m}}\cos\varphi_{\mathrm{ldj}}}$	(3.8)	$\varphi_3 = \mathrm{arctg}\dfrac{\sqrt{a}\omega L_2\cos\varphi_{\mathrm{ldj}}}{(1 - D_3)^2 Z_{\mathrm{ld}}^2 - \sqrt{a}\omega L_2\sin\varphi_{\mathrm{ldj}}}$	(3.25)
$U_{1\mathrm{m}} I_{1\mathrm{m}}\cos\varphi_1 = I_{\mathrm{ldm}}^2 R_{\mathrm{ld}}$	(3.9)	$I_{1\mathrm{m}} =$ $= \sqrt{U_{\mathrm{C1m}}^2\omega^2 C_1^2 + 2U_{\mathrm{C1m}}\omega C_1\frac{I_{\mathrm{ldm}}\sqrt{a}}{1 - D_3}\sin\varphi_{\mathrm{ldj}} + \frac{I_{\mathrm{ldm}}^2 a}{(1 - D_3)^2}}.$	(3.26)
$\Delta I_{\mathrm{L2}} = \dfrac{(U_{1\mathrm{m}} - U_{\mathrm{ldm}})D_1}{L_2 f_{\mathrm{m}}} = \dfrac{U_{1\mathrm{m}} D_1(1 - D_1)}{L_2 f_{\mathrm{m}}}$	(3.10)	$U_{\mathrm{C1m}} = U_{1\mathrm{m}} - I_{1\mathrm{m}}\omega L_1$	(3.27)

Continuation of Table 3.1

Buck action option

$$L_2 = \frac{U_{1m} D_1 (1 - D_1)}{(0.1 \ldots 0.2) I_{ldm} f_m} \quad (3.11)$$

$$\Delta U_{C2} = \frac{\Delta I_{L2}}{8 C_2 f_m} \quad (3.12)$$

$$C_2 = \frac{\Delta I_{L2max}}{8 \cdot 0.01 U_{1m} f_m} \quad (3.13)$$

$$\Delta U_{C1} = \frac{I_{L1m}(1 - D_1)}{C_1 f_m} \quad (3.14)$$

$$C_1 = \frac{I_{L1m}(1 - D_1)}{0.02 U_{1m} f_m} \quad (3.15)$$

$$\Delta I_1 = \frac{\Delta U_{C1}}{8 L_1 f_m} \quad (3.16)$$

$$L_1 = \frac{\Delta U_{C1max}}{8 \cdot 0.01 I_{1m} f_m} \quad (3.17)$$

Boost action option

$$\Delta I_{L2B} = \frac{D_3 U_{C1m}}{L_2 f_m} \quad (3.28)$$

$$L_{2B} = \frac{D_{3max} U_{1m}}{0.2 I_{ldmB} f_m} \quad (3.29)$$

$$\Delta U_{C2B} = \frac{(I_{L2B} - I_{ldmB})(1 - D_3)}{C_2 f_m} = \frac{I_{ldmB} D_3}{C_2 f_m} \quad (3.30)$$

$$C_{2B} = \frac{D_3}{0.05 Z_{ld} f_m} \quad (3.31)$$

φ_{ld} – shift angle between load voltage and current;
$\omega = 2\pi f$ – angular rotation frequency of vector diagram vectors;
I_{L2m} – amplitude of current flowing in inductance L2;
$a = Z_{ld}{}^2 \omega^2 C_2{}^2 - 2\omega^2 C_2 L_{ld} + 1$, Z_{ld};
φ_{ldj} – phase shift angles between inductor L2 current and load voltage;
i_{fM} – instantaneous input filter L_1C_1 current;
D_1 – filling factor for switching S1 on/off;
U_{2M} – voltage on switch S2;
U_{2Mm} – voltage amplitude on switch S2;
U_{ldm} – load voltage range;
$\tan\varphi_2$ – phase shift angle between u_{2M} and load voltage;
I_{1m} – amplitude of source current i_1;
φ_1 – phase shift angle between i_1 and input voltage source;
ΔI_{L2} – change of inductor L2 current in 1 modulation period;
ΔU_{C2} – amplitude of voltage change on capacitor C2;
ΔU_{C1} – amplitude of voltage change on capacitor C1;
ΔI_1 – amplitude of input current change;
i_{S4MB} – RMS value of the first harmonic of the current wave of switch S4;
I_{S4MmB} – maximum value of the first harmonic of the current wave of switch S4;
I_{L2mB} – amplitude of the first harmonic of the current in inductance L2;
U_{S3MmB} – amplitude of the first harmonic of the voltage on switch S3;
U_{C1m} – voltage of capacitor C1;
φ_3 – phase shift angle between voltage on capacitor C1 and switch S3;

ΔI_{L2B} – ripple of inductor L2 current first harmonic (boost mode);
L_{2B} – recommended inductance of inductor L2;
ΔU_{C2B} – voltage ripple to C2 (boost mode);
C_{2B} – capacitor C2 capacity (in boost mode).

Simulation results for boost mode are shown in Fig. 3.3.

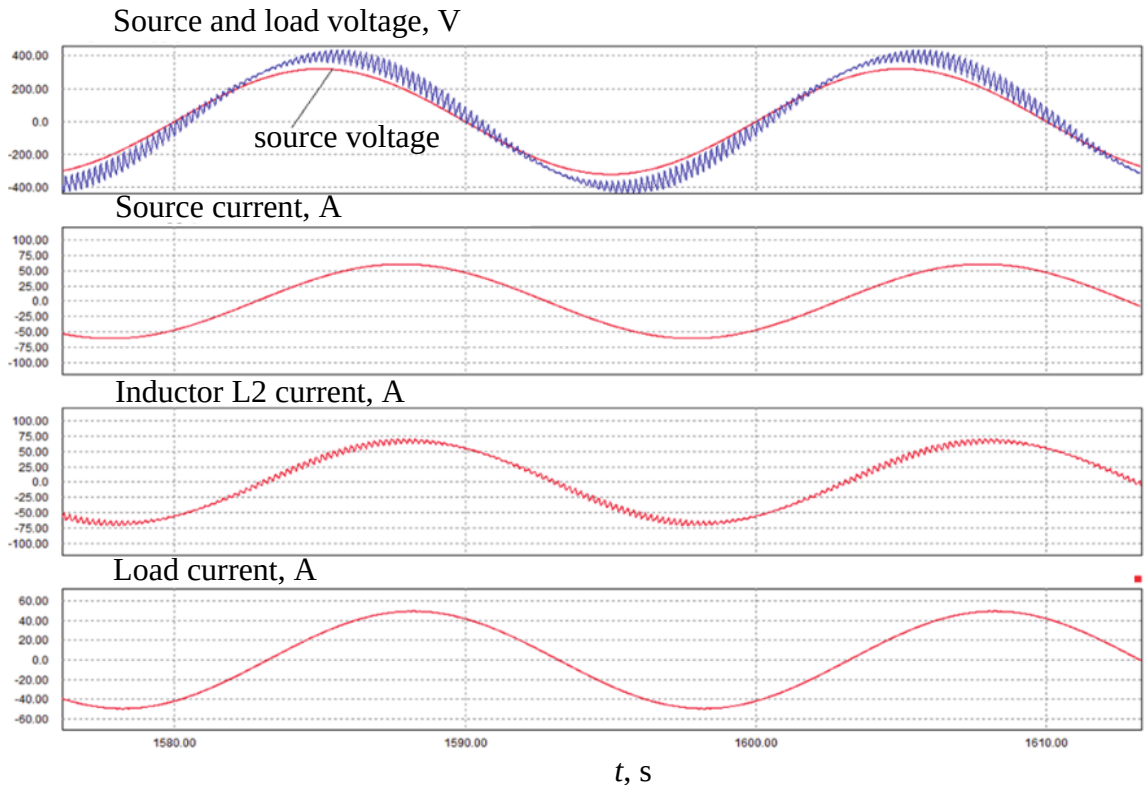

Fig. 3.3. Simulation results for boost mode L_1 = 1 mH; L_2 = 1.5 mH; C_1 = 90 μF; C_2 = 25 μF.

3.2. Efficiency of Using Advanced Buck–Boost Pulse Regulators

The circuit described above can be used to compensate voltage drops and surges by the help of IT.

The graphs obtained in the simulations (Fig. 3.5) show that by operating the closed AC/AC converter in the IT primary winding in boost mode, voltage drops can be compensated, even if input voltage reaches only 20 % (80 % voltage drop) of the nominal input voltage value.

Figure 3.6 shows the output voltage of the circuit shown in Fig. 3.4 if the AC/AC converter connected in parallel with its IT primary winding was operating in buck mode. Buck mode can be used in this case for the purpose of setting a more accurate output voltage because changing the existing IT transformation coefficient *D* from 0.1 to 0.9 gives an output voltage that changes only in the amplitude of 24 V if the input voltage is 230 V.

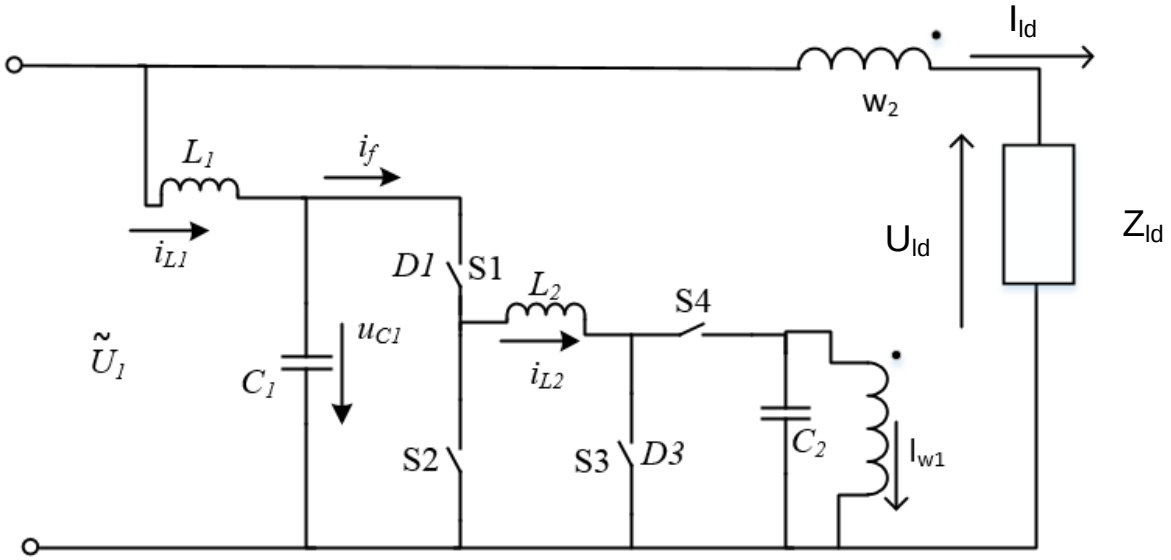

Fig. 3.4. Voltage stabilizer with IT primary winding connected AC/AC regulator with boost functionality.

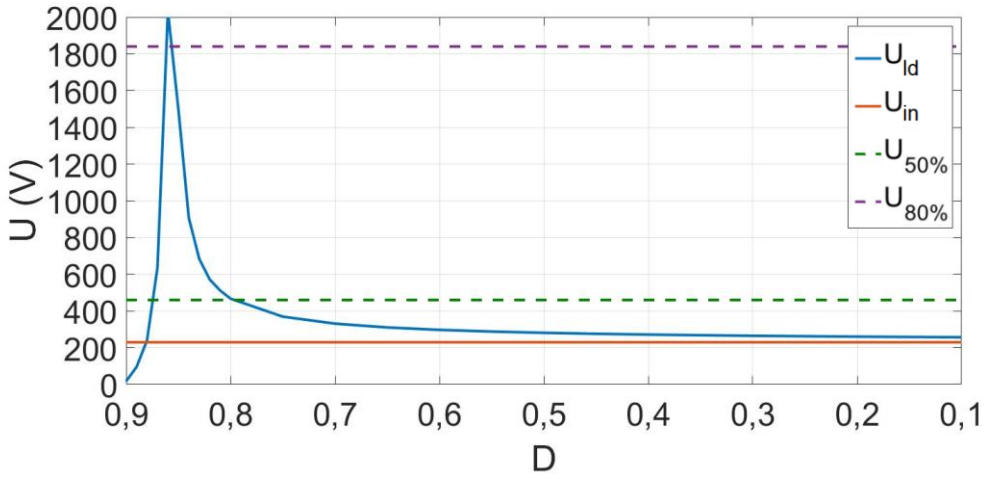

Fig. 3.5. Variation of the output voltage depending on the fill factor *D* when an AC/AC converter is connected to the IT primary winding and is operating in boost mode.

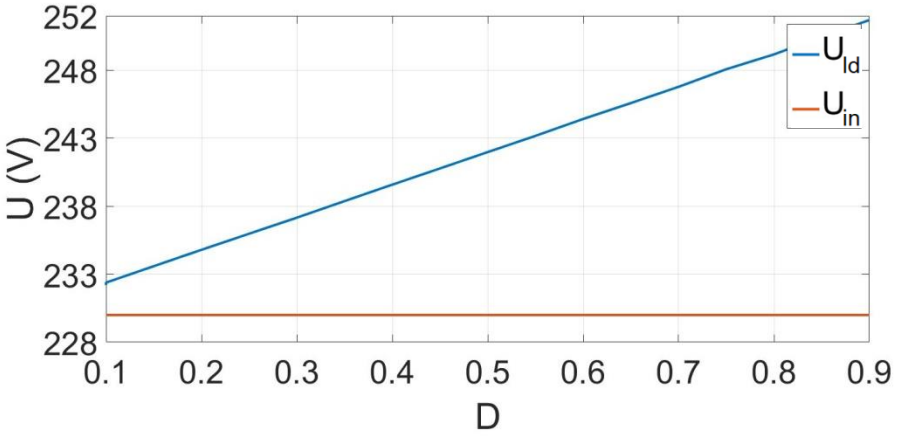

Fig. 3.6. Variation of the output voltage depending on the filling factor *D* when an AC/AC converter is connected to the IT primary winding and is operating in buck mode.

Looking more closely at Fig. 3.5, the question arises about the operation of the scheme when the fill factor *D* is greater than 0.85. In these moments, with the specific parameters, a shift was formed between the phase of the input voltage and the phase of the voltage at the IT output. The phase shift angle depending on *D* is shown in Fig. 3.7.

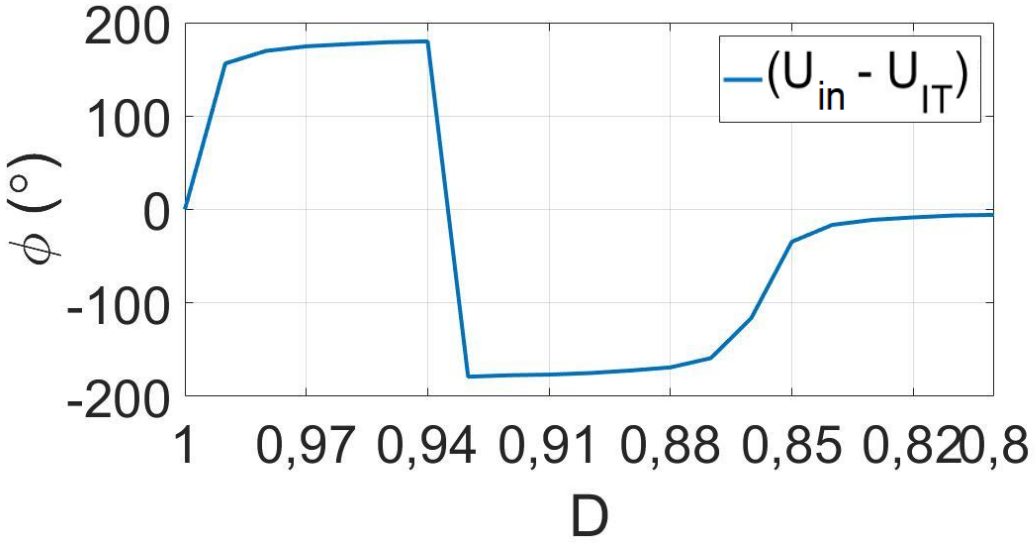

Fig. 3.7. The difference between the phases of input voltage U_{in} and the phases of the IT output voltage U_{IT}.

It can be concluded that the phases of voltage signals are opposite in the range of 0.99 to 0.94 and 0.93 to 0.88. This means that in addition to the introduction of additional switches in the circuits voltage surges can also be compensated.

Voltage surge compensation options when operating the AC/AC converter in the IT primary winding in boost mode, but with high *D* values, is shown in Fig. 3.8. AC/AC regulator input and output voltages in the case of 80 % voltage drop are shown in Fig. 3.9.

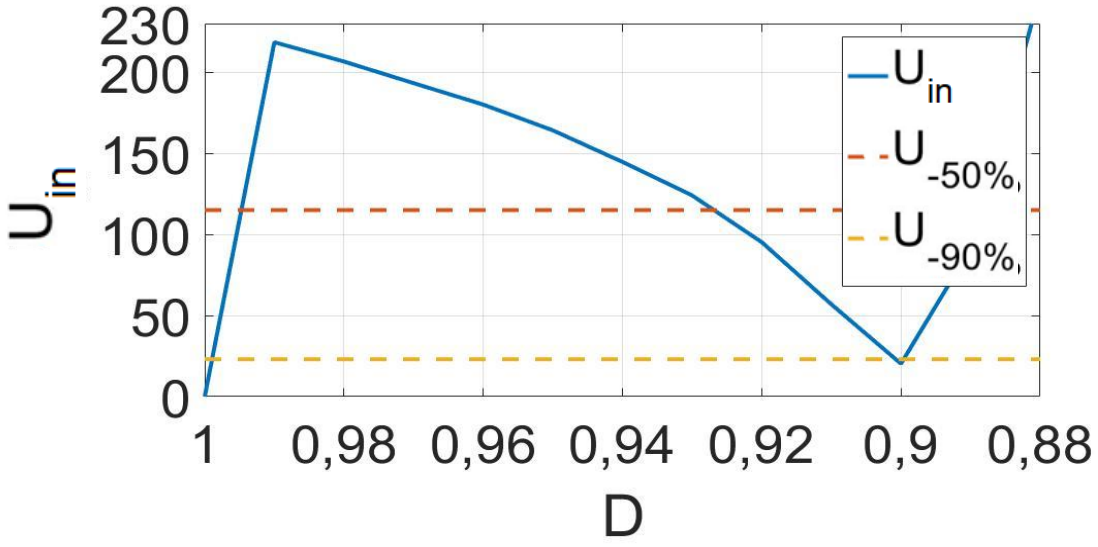

Fig. 3.8. Voltage surge compensation options when operating the closed AC/AC converter in the IT primary winding in boost mode but with high *D* values.

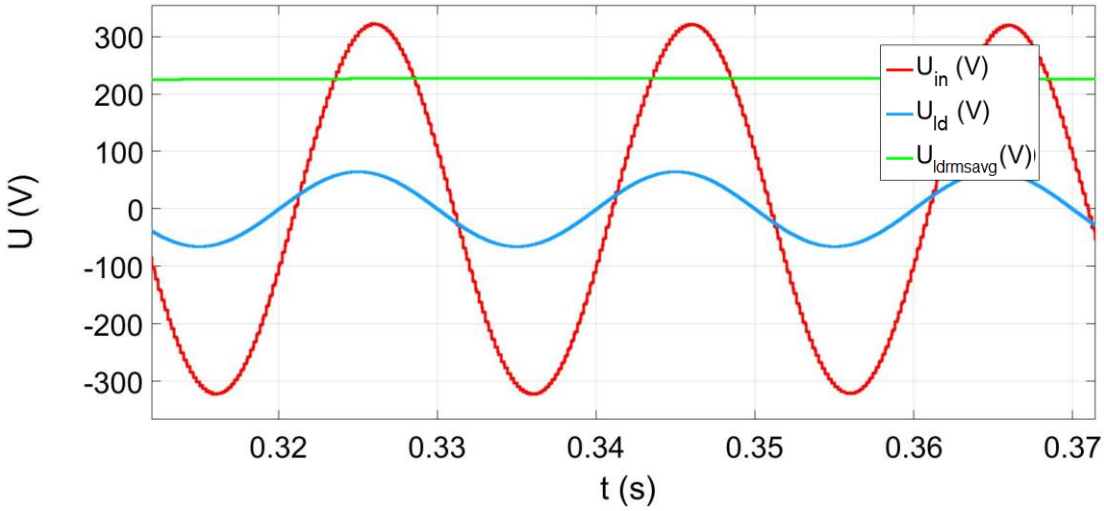

Fig. 3.9. Input voltage compensation in the case of 80 % voltage drop.

3.3. Phase Shift Angle Compensation

Using the scheme shown in Fig. 2.6 correction of the load voltage phase shift angle β can also be realized (Fig. 3.10 and 3.11). This need can arise both during voltage disturbance compensation and when it is simply necessary to connect two different stages of an electrical circuit that do not have the same phase shift angles and amplitudes.

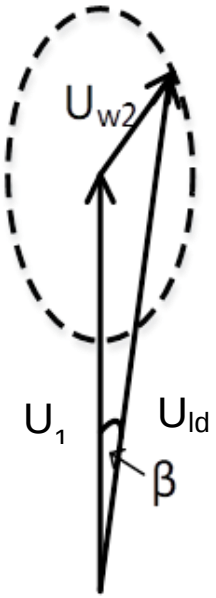

Fig. 3.10. Correction of the load voltage phase shift angle.

In order to obtain the fundamental harmonic of the time-delayed load signal, in the case of single-phase AC, in the bipolar modulation variant, $U_v > 0$ (i.e. $D > 0.5$) is set in each half-period with delay angle α.

Since direct connections are made when $U_v > U_z$ (D interval) and reverse when $U_v < U_z(1 - D)$, then at $U_v > 0$ a total voltage curve $U_{ld} = U_1(2D - 1)$ is formed in both U_1 positive and in the negative half (see Fig. 2.6), moreover, the connections are mostly direct because $D > 0.5$.

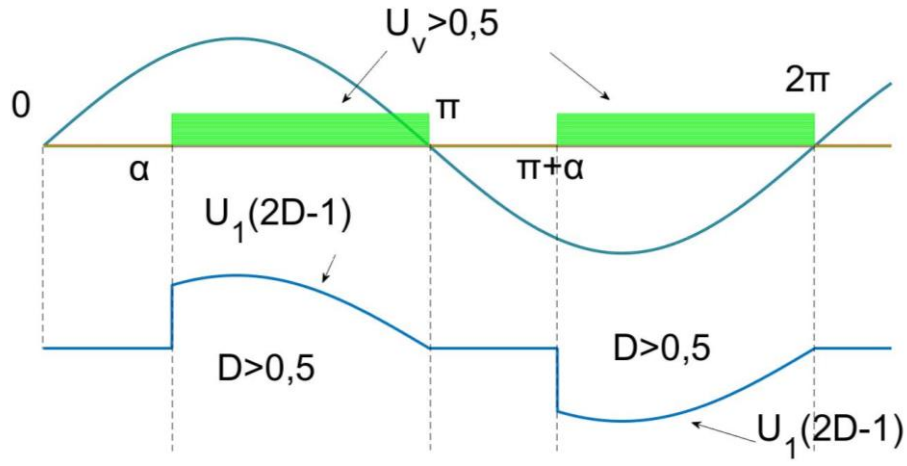

Fig. 3.11. Generation of the phase shift angle ahead of the supply voltage wave.

When $U_v > 0$, the direct connection gives DU_1 "mean wave" but the reverse – $(1 - D)U_1$ and together $U_{ld} = (D - 1 + D) = (2D - 1)U_1$. The basic harmonic of the load voltage is formed with amplitude $U_{ld(1)m} = U_{1m}(2D - 1)/(\pi\sqrt{A_1^2 + B_1^2})$, where A_1 is the amplitude of the sine component, B_1 is the amplitude of the cosine component. They are set in Table 3.2. A_1 and B_1 are calculated at different α. A graphical representation of the load voltage depending on parameters α and D is shown in Fig. 3.12. The fundamental harmonic shift angle $\varphi_{(1)}$ can be determined as $\text{arctg}\varphi_{(1)} = B_1/A_1$ (shown in Table 3.2).

$$A_1 = \frac{U_{1m}(2D-1)}{\pi}\left(\pi - \alpha + \frac{\sin 2\alpha}{2}\right); \tag{3.32}$$

$$B_1 = \frac{U_{1m}(2D-1)}{\pi}\left(\frac{1-\cos 2\alpha}{2}\right). \tag{3.33}$$

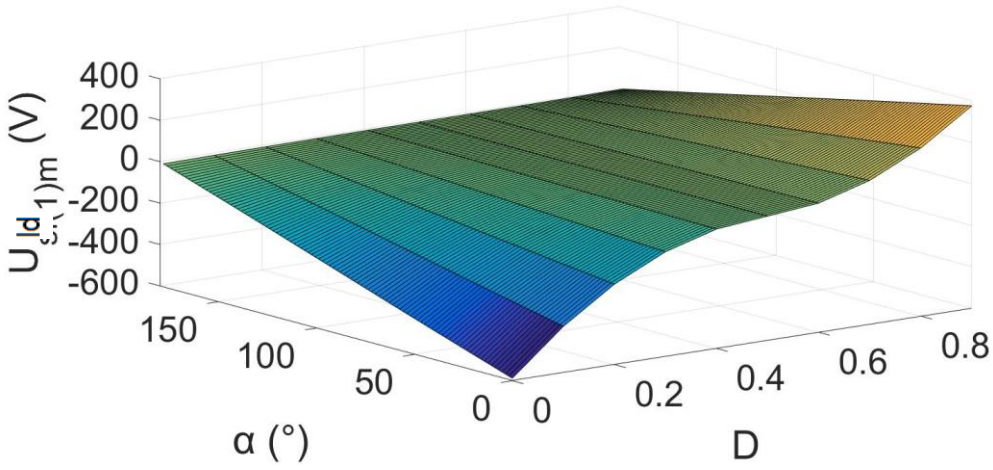

Fig. 3.12. Load voltage dependence on α and D.

Table 3.2

Phase shift angle depending on the control signal angle α in the case when a wave overtaking the phase of the source voltage is generated

α	**0°**	**30°**	**60°**	**90°**	**120°**	**150°**
A_1	π	3.05	2.53	π/2	0.61	0.09
B_1	0	–0.25	–0.75	–1	–0.75	–0.25
$\sqrt{A_1^2+B_1^2}$	π	3.06	2.64	1.86	0.967	0.265
$\varphi_1 = \text{arctg}\frac{B}{A}$	0°	–4.68°	–16.5°	–32.5°	–50.9°	–70.2°

To obtain a leading wave (Fig. 3.13), a pause of length α is introduced in each half-period; A_1 and B_1 at different offset angles are shown in Table 3.3.

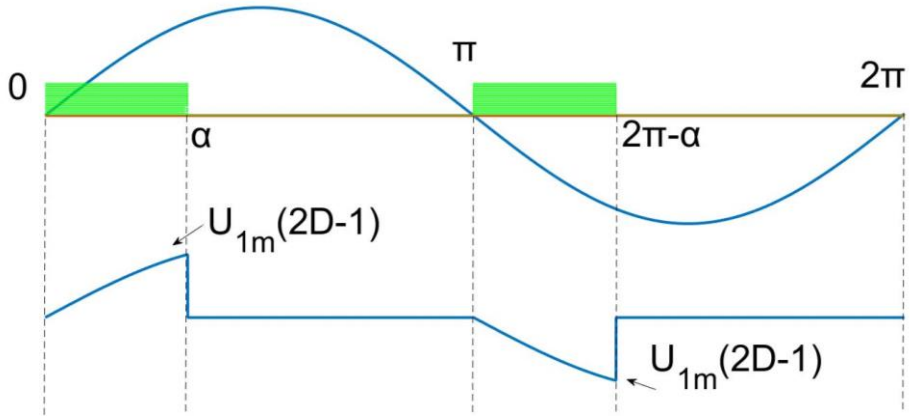

Fig. 3.13. Generation of IT primary winding signal lagging behind the supply voltage wave phase.

$$A_1 = \frac{U_{1m}(2D-1)}{\pi}\left[\pi - \alpha - \frac{\sin(-2\alpha)}{2}\right]; \tag{3.34}$$

$$B_1 = \frac{U_{1m}(2D-1)}{\pi}\left(\frac{\cos 2\alpha - 1}{2}\right). \tag{3.35}$$

Table 3.3

Phase Shift Angle Depending on the Control Signal Angle α in the Case when a Phase Wave Lagging Behind the Source Voltage Signal is Generated

α	**0°**	**30°**	**60°**	**90°**	**120°**	**150°**
A_1	π	3.05	2.526	π/2	0.61	0.09
B_1	0	0.25	0.75	1	0.75	0.25
$\sqrt{A_1^2+B_1^2}$	π	3.06	2.64	1.86	0.967	0.265
$\varphi_1 = \text{arctg}\frac{B_1}{A_1}$	0°	4.68°	16.5°	32.5°	50.9°	70.2°

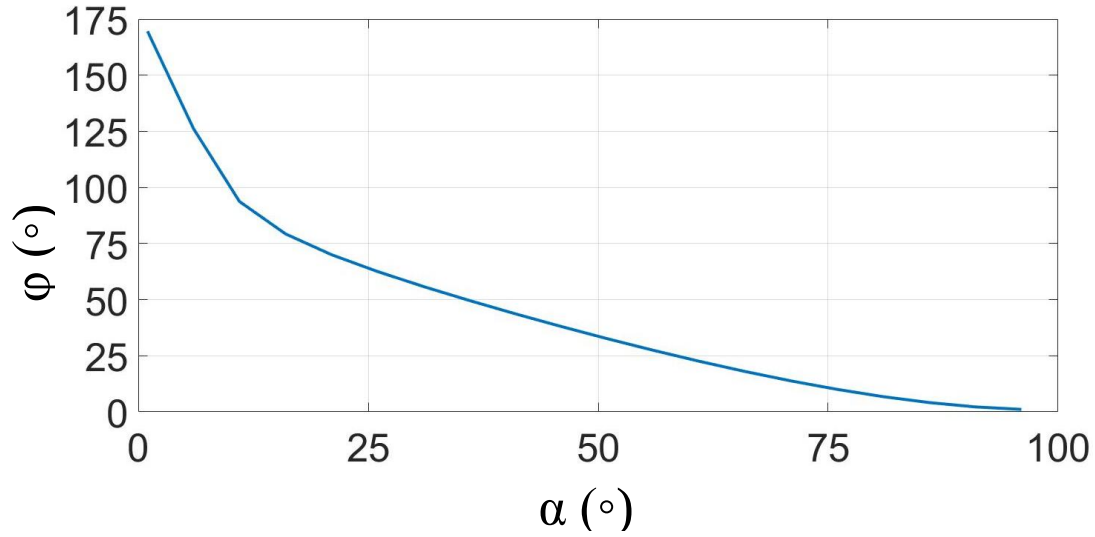

Fig. 3.14. Phase shift angle (in the negative direction) depending on the modulation angle α.

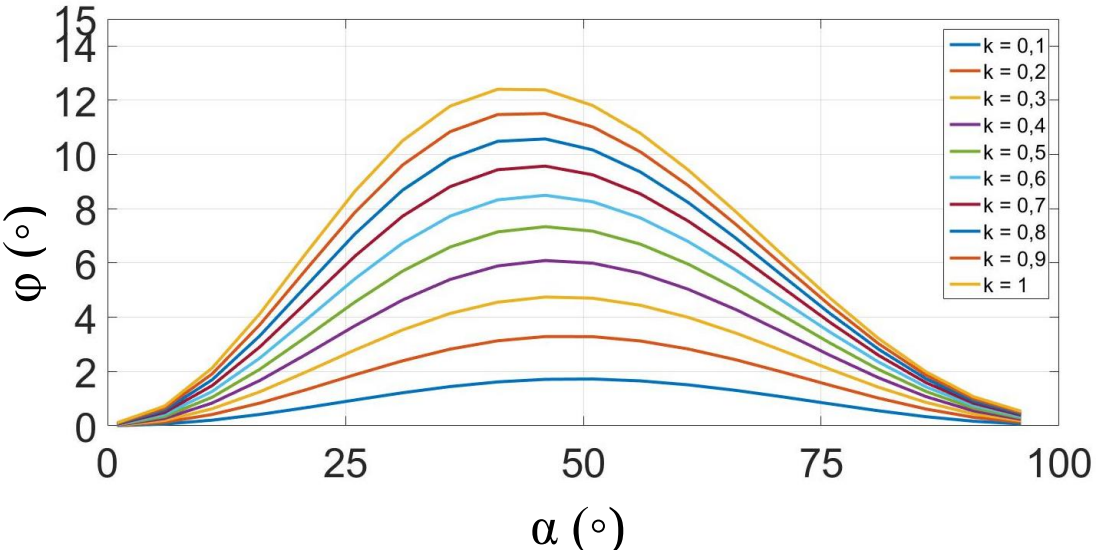

Fig. 3.15. Possibilities of load voltage phase shift angle correction (in the negative direction) depending on modulation angle α and the IT transformation coefficient *k*.

3.4. Interphase Modulation

In a three-phase voltage system, modulation can be performed by connecting the load alternately, for example, phases A and B; so, a direct connection is made alternately. When $U_v > U_z$ (bipolar sawtooth signal, see Fig. 3.16), then in the D interval U_A is connected to the load, when $U_v < U_z(1 - D)$ in interval, U_B is connected as shown in Fig. 3.14. Such a solution can be used, for example, to expand the possibilities of load phase shift angle correction. Figure 3.16 shows one of the possible operating principles of the control circuit – comparison of the sawtooth voltage with the set DC voltage with the help of a comparator.

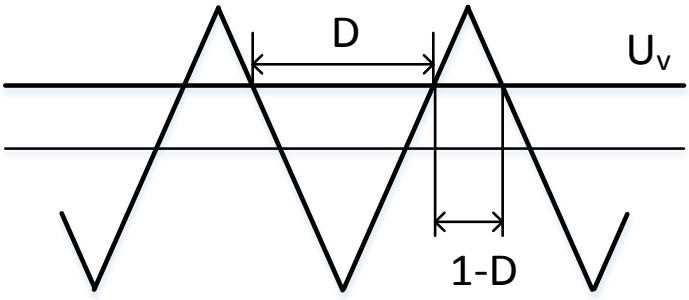

Fig. 3.16. Periods when phase switching may occur.

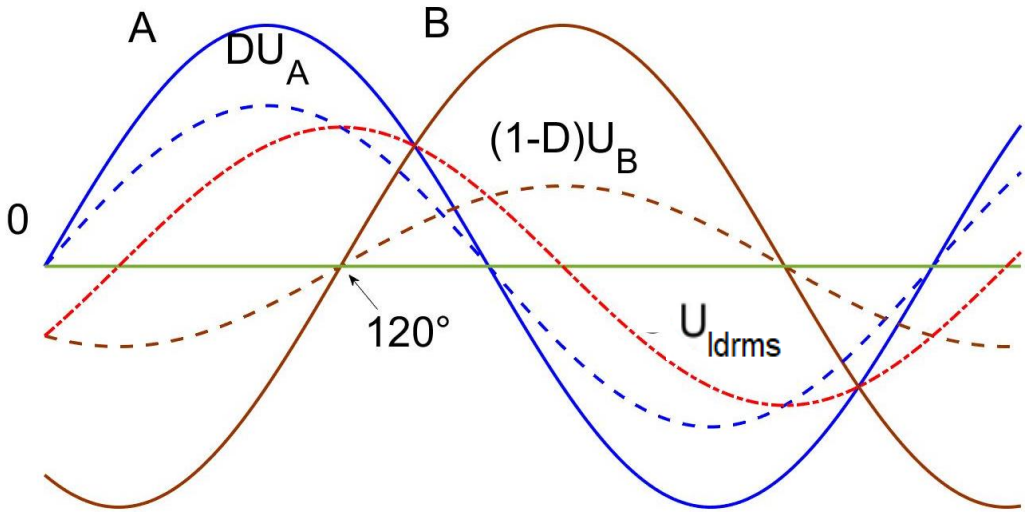

Fig. 3.17. Representation of the basic harmonic components of phases A and B as well as their modulated waves.

The resulting wave can be obtained using a vector diagram.

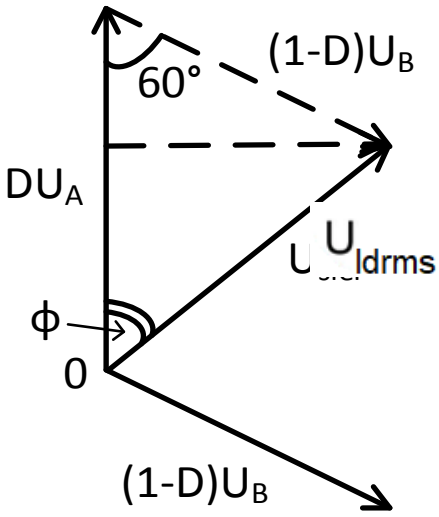

Fig. 3.18. Vector diagram for obtaining an IT wave from phases A and B.

$$U^2_{\text{ldrms}(1)} = (1-D)^2 U^2_{\text{B}} \sin^2 60° + [DU_{\text{A}} - (1-D)U_{\text{A}} \cos 60°]^2; \quad (3.36)$$

$$U^2_{\text{ld}(1)} = U^2_{\text{f}}(1 - 2.5D + 2.5D^2). \quad (3.37)$$

Offset angle to U_{A} vector

$$\text{tg}\varphi = \frac{(1-D)\sqrt{3}}{3D-1}. \quad (3.38)$$

You can easily change the offset angle φ and at the same time U_{slef}.

The resulting curve can also be obtained by summing the instantaneous DU_{A} and $(1 – D)U_{\text{B}}$ curves, the amplitude of the resulting curve being at an angle φ_0:

$$\text{tg}\varphi_0 = \frac{1-D}{\sqrt{3}(1-D)}. \quad (3.39)$$

Modulation of two-phase voltage signals can also be used to obtain a third-phase voltage signal, which can be useful in the event when one of the phases has had its power supply completely interrupted. One of the solutions are considered in [5] and [55].

3.5. Three Phase Voltage Regulation

As another solution offered in this work is seen in Fig. 3.4 – a circuit is connected in each phase and connected to a special IT circuit to provide voltage to each phase in case the voltage supply is still maintained in the other two phases. Using Fig. 3.19 the visible solution can compensate for 0–80 % voltage drops.

As a negative feature of this scheme, it should be mentioned that in case you want to make voltage corrections in each phase, then a total of six in Fig. 3.4 shown diagrams as well as three-winding Its are needed.

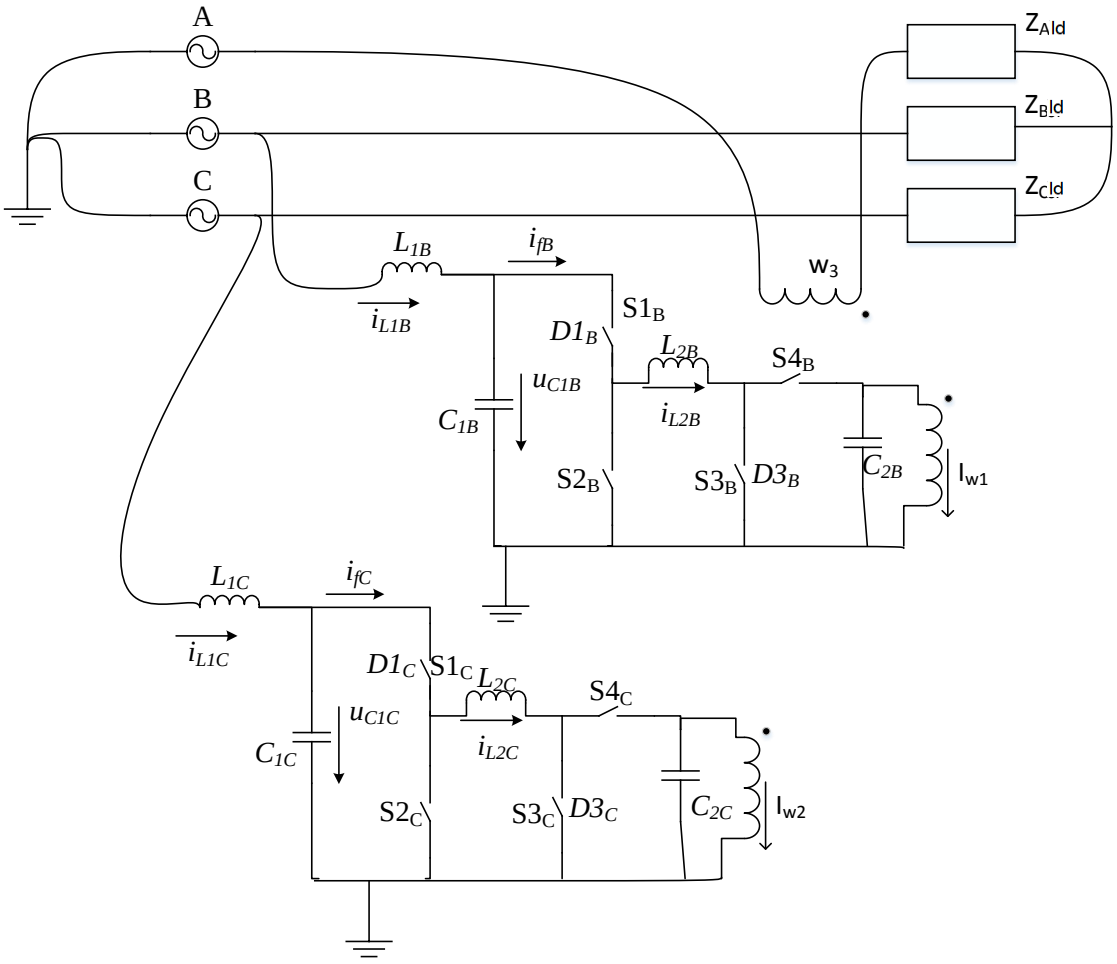

Fig. 3.19. Use of two-phase voltage modulation for the purpose of third-phase voltage correction.

Conclusions of Chapter 3

1. The scheme of buck–boost AC control system in the primary winding circuit is proposed. Its calculations are performed using the base harmonic method which shows high accuracy. If such a buck–boost system is connected to the primary winding circuit, the range of changes in the output load voltage can be significantly extended.
2. Of greatest interest is bipolar modulation, which allows to change not only the parameters of the load voltage but also its type (DC, AC) and phase shift angle.
3. A large number of semiconductor elements is required to regulate the three-phase voltage with the proposed method. It is possible to reduce the number of switches at the expense of reduced functionality.

4. PRACTICAL SOLUTIONS AND MODEL RESEARCH OF IT VOLTAGE REGULATORY SYSTEMS

4.1. Developed Voltage Stabilization Systems

Within the framework of the work, practical solutions have been developed for the purpose of in-depth research of voltage stabilization systems. A triac-driven solution as well as a transistor-powered solution [58] have been developed.

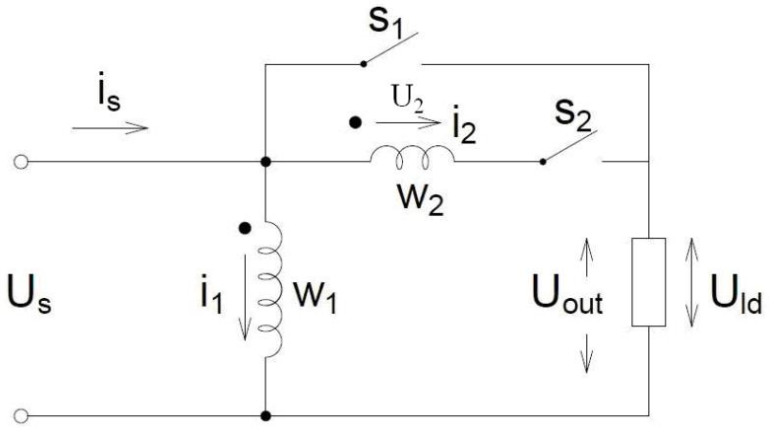

Fig. 4.1. Schematic representation of voltage regulator.

By using the operation of modulated switches S1 and S2, the RMS value of the load voltage can be changed smoothly. In the case of using triacs, the modulation period in the experiment with 50 Hz alternating current was 100 Hz, but in the case of using transistors the frequency 1 kHz was used in the experiment.

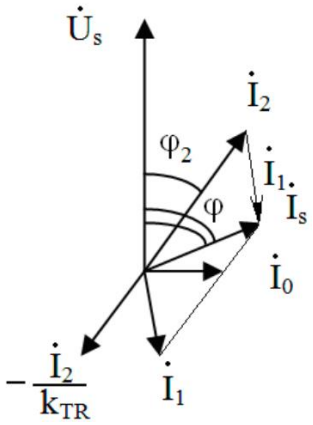

Fig. 4.2. Vector diagram for the circuit shown in Fig. 4.1.

The variant with triac control has been used in lighting intensity control circuits in a gas discharge lamp. And it has been found that the scheme achieves significant electricity savings in the event of a reduced voltage.

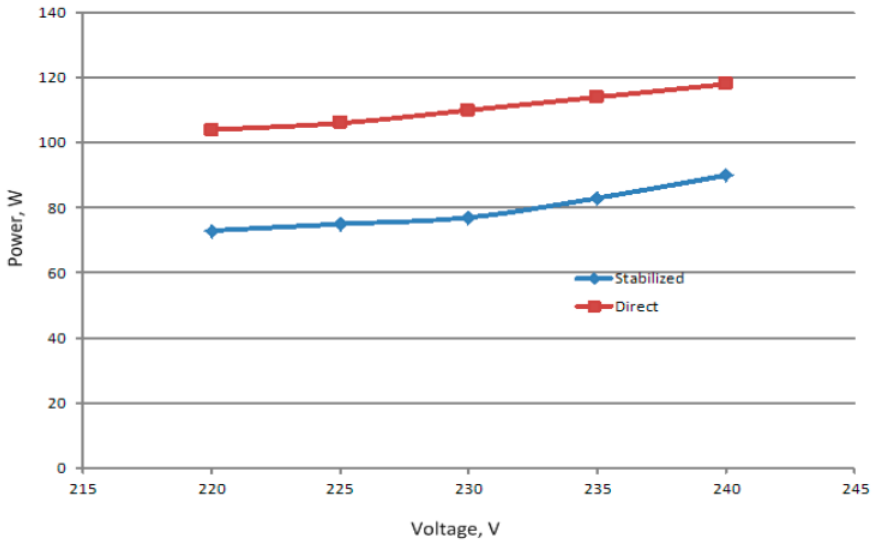

Fig. 4.3. Differences in gas discharge lamp power consumption between attempts without and with the use of a voltage regulator.

As can be seen in Fig. 4.3, energy savings of up to 25 % were achieved when using regulators. A similar experiment was performed with an asynchronous motor, whose current and voltage forms were taken, as well as electricity savings were obtained. The developed prototype of the controller with the used IT is shown in Fig. 4.4.

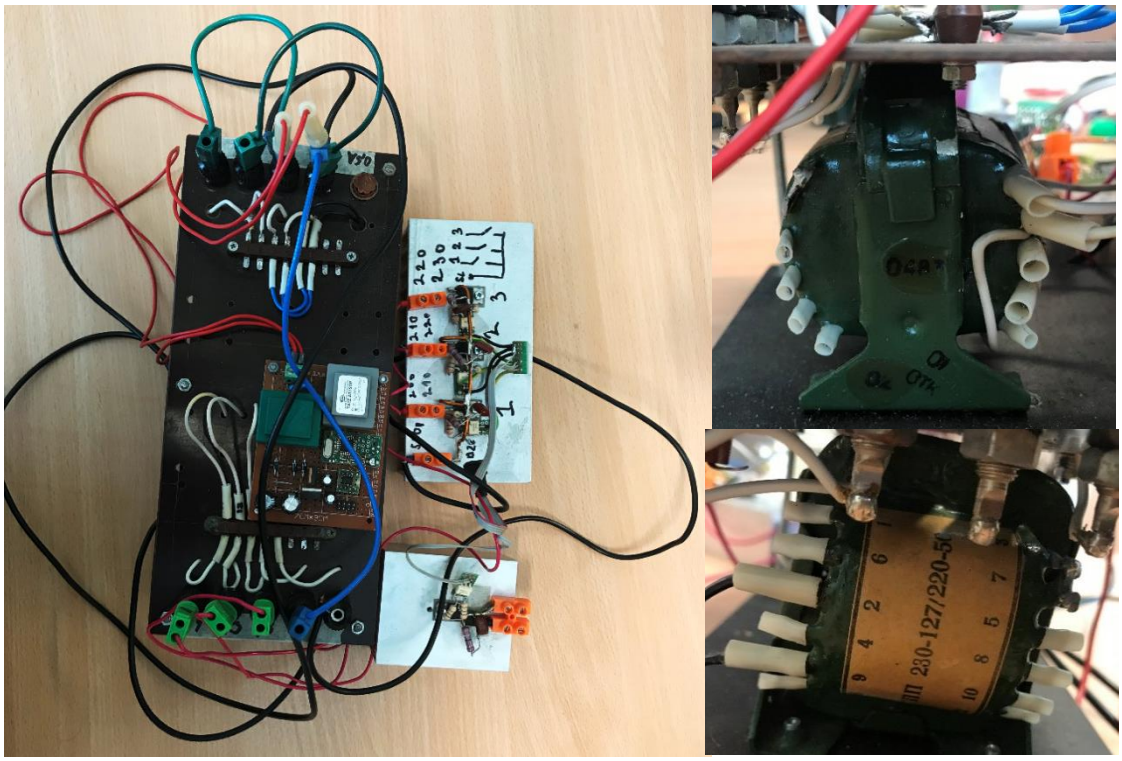

Fig. 4.4. Voltage regulator prototype.

The voltage regulator with voltage sag and swell compensation capability was developed on the basis of MOSFET (Fig. 4.5). Its efficiency was tested with an active load of up to 840 W.

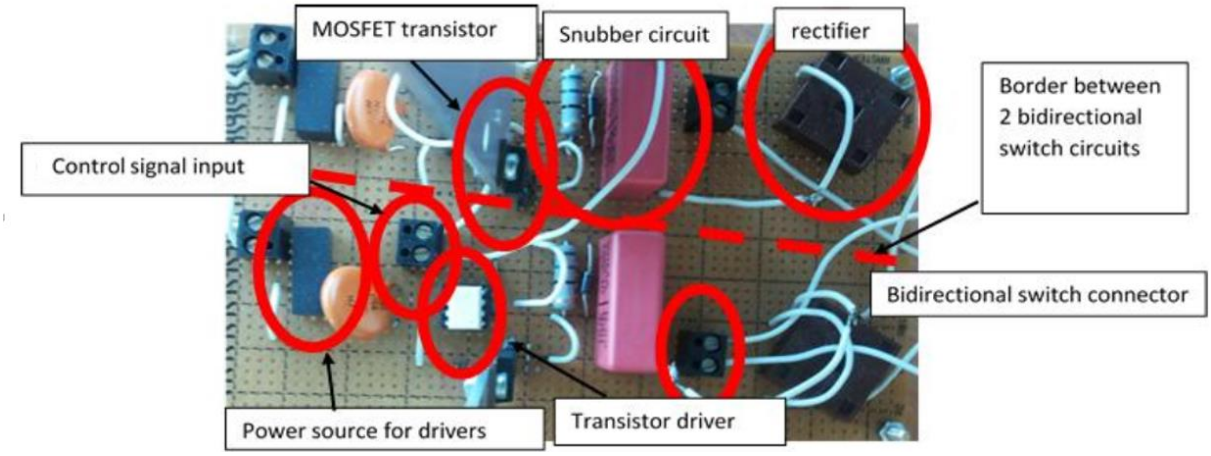

Fig. 4.5. Prototype of a voltage stabilizer based on MOSFET.

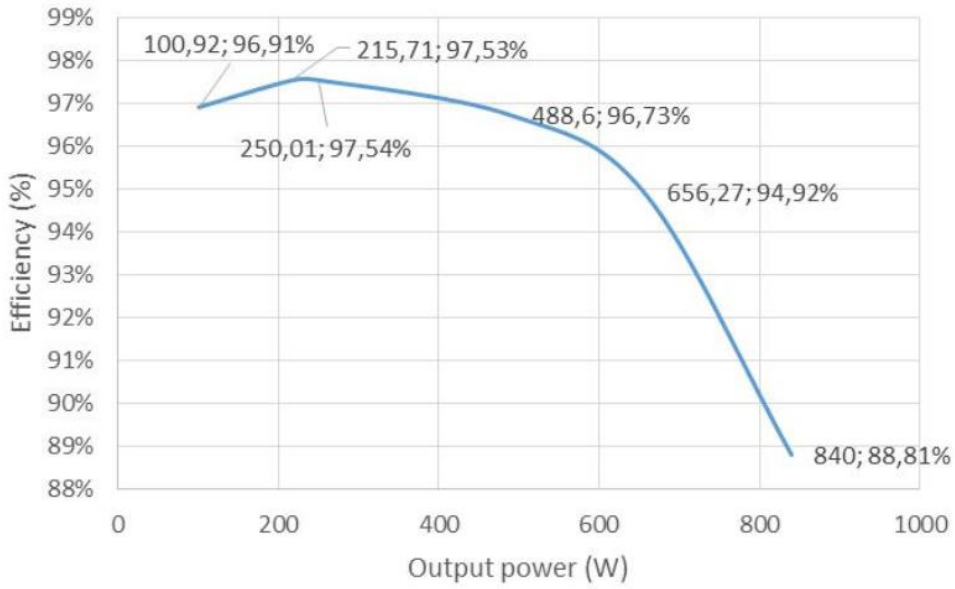

Fig. 4.6. Voltage stabilizer efficiency measurements with different active load values.

4.2. Converter of a Three-Phase System to Two-Phase System

Based on the defined principles of unipolar and bipolar AC modulation, several interesting technical solutions can be created. For example, the application of bipolar AC modulation to a single-phase voltage allows to create a reversible single-phase rectifier that can be adjusted by changing the basic harmonic amplitude of the modulated voltage (Fig. 4.7).

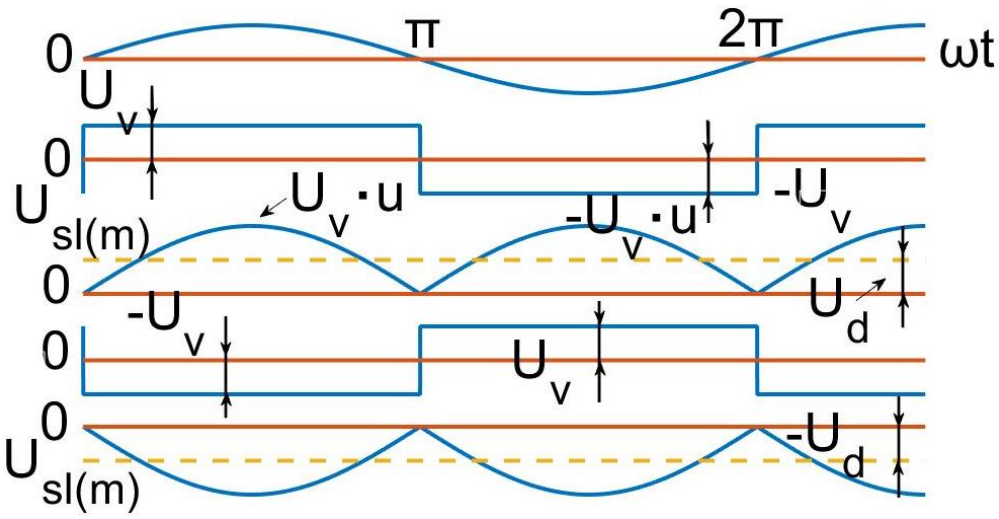

Fig. 4.7. Voltage signals at the input and output of an adjustable and reversible single-phase rectifier (also control signal).

Assuming for control purposes a bipolar saw voltage with frequency $2f$ and amplitude U_{zm}, and applying a positive control voltage U_v in the positive half-period of the source voltage and negative polarities $-U_v$ in the negative half-period u, in the range from 0 to π the predominance of the direct connection intervals is formed on the load, and respectively the positive polarity "mean" voltage half-wave, but from π to 2π – the predominance of the negative connection is formed, and on the load – also the positive polarity "mean" wave.

In the time interval from 0 to π, the direct connection lasts relatively long during the modulation period:

$$D_{0\pi} = 0.5\left(1 + \frac{U_v}{U_{zm}}\right), \tag{4.1}$$

and the "mean" wave of this connection voltage is formed as

$$u'_{Mt} = 0.5U_m\left(1 + \frac{U_v}{U_{zm}}\right)\sin\omega t. \tag{4.2}$$

But the relative connection lasts relatively long:

$$(1 - D_{0\pi}) = 0.5\left(1 - \frac{U_v}{U_{zm}}\right), \tag{4.3}$$

and

$$u'_{MR} = 0.5U_m\left(1 + \frac{U_v}{U_{zm}}\right)\sin\omega t. \tag{4.4}$$

As a result, a voltage M wave is formed from 0 to π:

$$u'_M = u_{tM} - u_{RM} = U_m\frac{U_v}{U_{zm}}\sin\omega t = U_m U_v^*\sin\omega t. \tag{4.5}$$

In the second half, $u_v = -U_v$, the direct connection lasts:

$$D_t'' = 0.5\left(1 - \frac{U_v}{U_{zm}}\right); \tag{4.6}$$

and reverse

$$D_R'' = 1 - D_t'' = 0.5(1 + U_v^*). \tag{4.7}$$

As a result

$$u_{(M)}'' = -U_v^* U_M \sin \omega t, \tag{4.8}$$

where $\pi \leq \omega t \leq 2\pi$ and $u_{(M)}'' > 0$.

The rectified value is

$$U_d = 0.9 U_v^* U_{rms}, \tag{4.9}$$

where U_{rms} is value of the effective voltage of the source.

Since U_v* can change the sign, the rectifier is reversible – depending on the U_v* sign in the positive half-cycle of the source voltage, the polarity of the TQ voltage changes.

Using such a rectifier, it is possible to realize a transformer-free DC input unit for various electrical equipment – dimmable electrical equipment, lighting bulbs, power supply equipment, etc. – and in different technologies.

The AC modulated voltages in the electric drive can be used to control the starting, reversing and braking processes of AC electric motors.

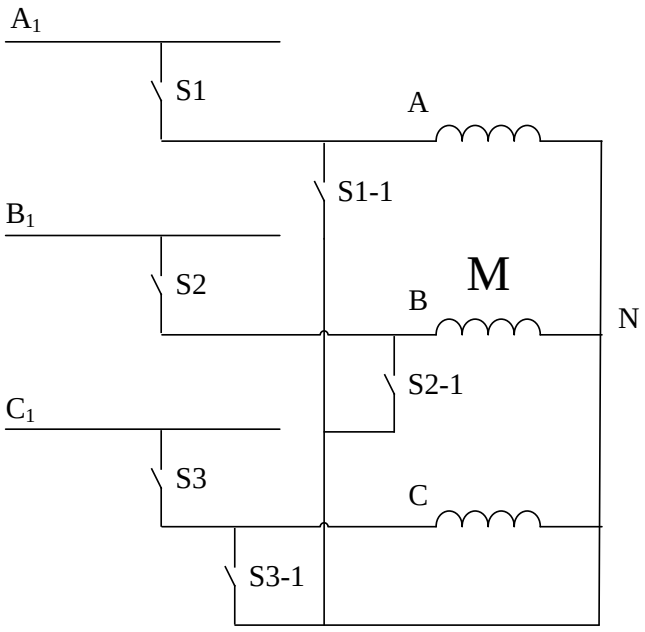

Fig. 4.8. Setup of smooth start asynchronous motor.

If unipolar modulation pulse regulators are introduced between all 3 AC phases (Fig. 4.8), then by changing the control voltage, the voltage on the windings of the asynchronous electric motor can be smoothly increased, thus achieving a “soft” start:

$$U_{\text{fm}} = U_{1\text{f}}D = U_{1\text{f}}\frac{U_{\text{v}}}{U_{\text{zm}}}, \tag{4.10}$$

where the control must use a unipolar sawtooth signal with amplitude U_{zm}. If the phase winding outputs of the asynchronous electric motor are freely available, then by applying bipolar modulation pulse control between the 3 phases of the power supply the phase windings can be provided with both a voltage increase and a phase sequence (A constant, B and C rotated back and forth by 120°, respectively), but by introducing a single-phase TQ control for each phase, providing dynamic braking.

Phase inversion can be of poor quality without providing the same amplitude for all 3 voltages.

Using bipolar modulation, each single-phase voltage rectification situation of one phase can be repeated *N* times, and in such a way the basic harmonic of the voltage on the load with a reduced frequency of *N* times can be obtained. It can create a cycloconverter of AC voltage, actually dividing the frequency of the power supply by *N* (Fig. 4.9)

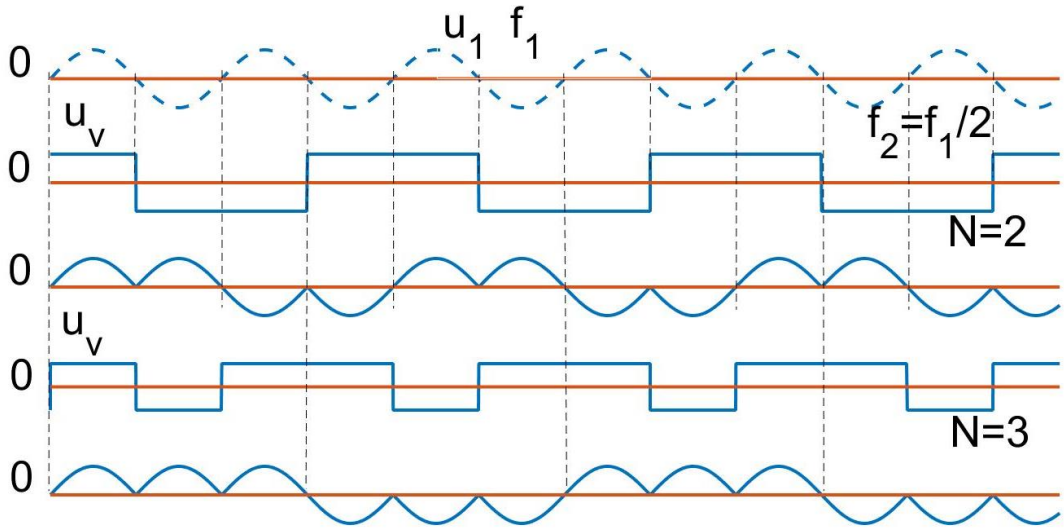

Fig. 4.9. By modulating the voltage of one phase, the output voltage shapes of the converter are obtained.

If 2 such bridge pulse regulators are created from one supply phase, then by shifting the control signals both by 90° in phase we will get 90° shifted voltages u_2, which could be connected to both phases of the two-phase induction motor (if they are not electrically connected), and by adjusting *N*, control the speed of the two-phase electric motor down from rated.

In addition, by changing the phase shift between u_{v1} and u_{v2}, a reversal of $N = 2$ can be realized; u_{v2} lags behind u_{v1} by 90°.

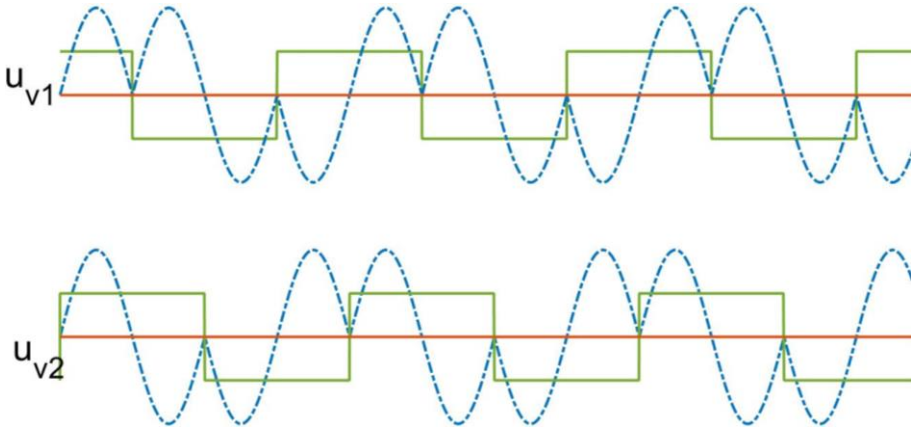

Fig. 4.10. Creation of two phases from one phase.

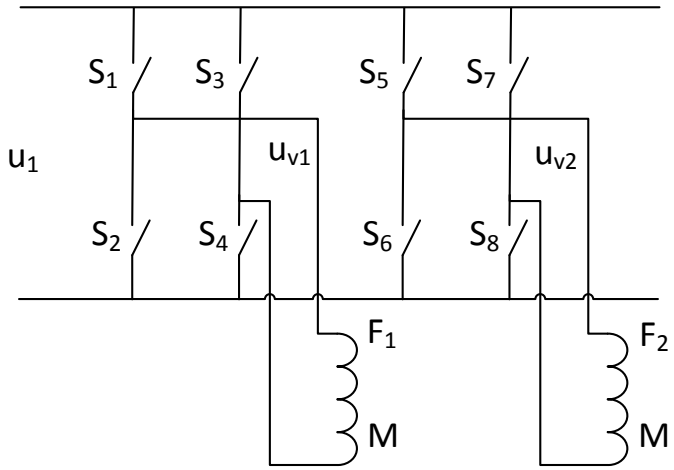

Fig. 4.11. Two-phase system modulator.

Similarly, a 3-by-120° offset control signal system can be set up and single-phase to three-phase cycloconversion can be performed using a total of 12 bidirectional control switches.

Due to the problems of bipolar modulation, it is difficult to create a common zero point for several loads. Therefore, in cases where a common zero point is required, the third principle of AC modulation – interphase modulation – should be applied.

For example, splitting a single-phase voltage into a two-phase voltage with a 90° phase shift can be realized in Fig. 4.12 in which the voltages of phases A and B (respectively D and $1 - D$ intervals in modulation period $1/f_m$) are connected alternately to the load of phase A' to obtain the new phase A'.

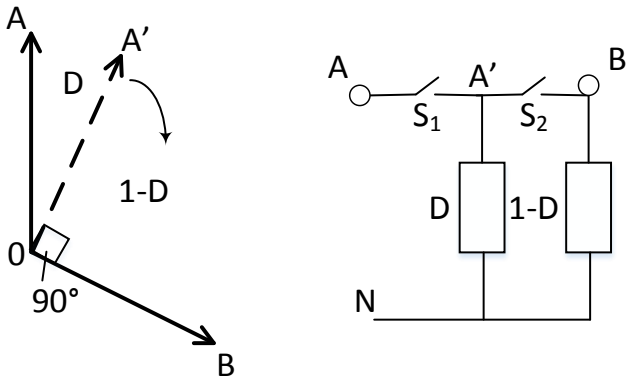

Fig. 4.12. Single-phase voltage splitting with a 90° offset.

Thanks to the capacitor, the angle between phases 10 and 20 is close to 120°, and the angle between phases 30 and 20 is close to 90°. By introducing interphase modulation between 30 and 10, a new vector 30 can be obtained, which will be offset by 120° with respect to 20. Interphase modulation can be used to obtain a three-phase control vector system that could be used both in technological processes and to control the speeds of electric motors.

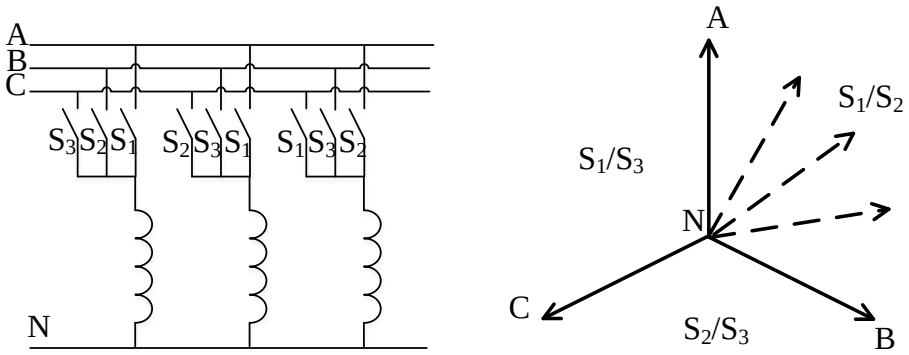

Fig. 4.13. Implementation of phase shift in a three-phase system with the help of two-way semiconductor switches.

Conclusions of Chapter 4

1. The developed voltage stabilization system is used for the purpose of voltage reduction, and stabilization can reduce both the number of equipment disconnections and the electricity consumed by them (both active and reactive).
2. A combination of four bidirectional switches with different control methods has found a number of different applications, proving that if there were affordable two-way semiconductor switches, they would be in demand.
3. The use of IT in combination with the implementation of a cycloconverter with bidirectional switches results in significant improvements in voltage THD.

CONCLUSIONS

1. Modern IT control methods are based on system voltage high frequency modulation solutions with the help of semiconductor switches.
2. In-depth research of pulse modulation techniques of alternating current quantities is the basis of research of IT systems; they have an important independent role in creating various solutions even without IT.
3. The power of the control circuit can be 10 times less than the load power if it is planned to regulate the change of the output voltage in the range of 10 %.
4. The direct result of pulse modulation of AC signals must be sought in the form of **base-harmonic** parameters of modulated voltage and current signals (amplitude, RMS value, phase shift angle) which determine the parameters of almost sinusoidal type inductive circuits associated with the first type modulated signals and capacitive circuits of almost sinusoidal voltage type signal parameters.
5. Due to the pulse modulation of AC signals, it is possible to create various voltage stabilization and reactive power correction devices on the IT primary or secondary winding.
6. Using the proposed system, it is possible to achieve up to 25 % energy savings in street lighting systems operated by gas discharge lamps.
7. The number of semiconductor switches in a circuit designed to compensate for 80 % of voltage drops or surges due to the phase shift caused by reactive elements can be reduced to 2 semiconductor bidirectional switches while maintaining a small IT size.
8. The application of multiphase AC interphase pulse modulation allows to create phase-shifted new vectors, as well as to solve their spatial orientation problems.
9. In high-power systems, THD improvements can be effectively made with the help of injection transformer.
10. High-frequency modulation of AC circuits can be the basis for both advanced DC and AC technology with a variety of applications. One of the simplest and most efficient solutions is the introduction of injection transformers with high-frequency modulation stages, which allows to reduce the IT dimensions up to ten and several times against a completely low-frequency IT system. The involvement of such high-frequency unipolar and bipolar modulation elements for low-frequency on-load signal acquisition is an immediate technical task for various applications.

FUTURE WORK

During the development of the work, several direct AC/AC converters have been studied, which can be used to solve technical tasks such as voltage disturbance compensation, speed control of electric machines, change of the number of supply voltage phases and change of AC frequency. Although the study is extensive and has given good results, it has also led to the idea of an even broader study which would include an examination of extended control methods of the proposed solutions as well as supplementing it with nonlinear inductances [29], [61]. The study of literature revealed that the proposed solutions are particularly suitable for high supply voltages [76]. Therefore, an expanded scope of practical experiments would be needed to fully verify the proposed solutions.

BIBLIOGRAPHY

[3] J. M. Flores-Arias, A. Moreno-Munoz, R. Real-Calvo, J. R. Sanchez, "Transformerless power line voltage conditioner and regulator based on CA PWM Chopper," presented at 2010 IEEE International Symposium on Industrial Electronics, Bari, Italy, July 4–7, 2010.

[4] O. C. Montero-Hernhdez, P. N. Enjeti, "Application of a Boost AC-AC Converter to Compensate for Voltage Sags in Electric Power Distribution Systems," in *Proc. 31st Annual Power Electronics Specialists Conf.*, 2000. pp. 470–476.

[5] J. Kaniewski, P. Szczesniak, M. Jarnut and G. Benysek , "Hybrid Voltage Sag/Swell Compensators: A Review of Hybrid AC/AC Converters", *IEEE Industrial Electronics Magazine, vol. 9, issue 4, pp. 37–48, Dec.* 2015.

[7] E. C. Aeoliza, N. P. Enjeti, L. A. Moran, O. C. Montero-Hernandez and K. Sangsun, "Analysis and design of a novel voltage sag compensator for critical loads in electrical power distribution systems", IEEE Trans. Ind. Appl., vol. 39, no. 4, pp 1143–1150, July/Aug. 2003.

[9] S. Zahra, M. Siddique, J. Hussain, S. Jabbar, M. Riaz, "A new reliable Single-Stage Single-Phase AC-AC Converter based Dynamic Voltage Restorer for Voltage Sag/Swell compensation", in *Proc. 2020 3rd International Conference on Computing, Mathematics and Engineering Technologies (iCoMET)*, 2020. pp. 413–420.

[10] I. Rankis, M. Prieditis and G. Stana, "Investigation of dirrect AC-AC BUCK converter with series injection transformer," *2018 IEEE 59th International Scientific Conference on Power and Electrical Engineering of Riga Technical University (RTUCON)*, Riga, Latvia, 2018, pp. 1–6.

[11] Z. Wang and J. Wang, "Review on Implementation and Assessment of Conservation Voltage Reduction," in *IEEE Transactions on Power Systems*, vol. 29, no. 3, pp. 1306–1315, May 2014.

[12] Zhou Jing-hua, Chen Cheng, Zhang Xiao-wei and Chen Ya-ai, "Reducing voltage energy-saving control method of induction motor," *2013 International Conference on Electrical Machines and Systems (ICEMS)*, Busan, Korea (South), 2013, pp. 2159–2162.

[13] Seok-Il Go, S. Ahn, J. Choi, Won-Wook Jung and C. Chu, "Development and test of conservation voltage reduction application for Korean Smart Distribution Management System," *2015 IEEE Power & Energy Society General Meeting*, Denver, CO, USA, 2015, pp. 1–5.

[14] D. Shirkin and I. Rankis, "Transformer based AC pulse regulation systems," *2014 55th International Scientific Conference on Power and Electrical Engineering of Riga Technical University (RTUCON)*, Riga, Latvia, 2014, pp. 52–55.

[15] S. Martinez Garcia, J. C. Campo Rodriguez, J. A. Jardini, J. Vaquero Lopez, A. Ibarzabal Segura and P. M. MartÍnez Cid, "Feasibility of Electronic Tap-Changing Stabilizers for Medium Voltage Lines – Precedents and New Configurations," in *IEEE Transactions on Power Delivery*, vol. 24, no. 3, pp. 1490–1503, July 2009.

[16] N. F. Mailah, S. M. Bashi and W. H. Meng, “Microcontroller based semiconductor tap changer for power transformer,” *2003 IEEE Bologna Power Tech Conference Proceedings,*, Bologna, Italy, 2003, pp. 6, pp. Vol. 4.

[17] F.Q. Yousef-Zai and D. O'Kelly, “Solid-state on-load transformer tap changer,” in *IEE Proc. - Electric Power Applications*, Nov. 1996, pp. 481–491.

[18] J. Alvarez, R. Echavarria and A. Flores, “A fast regulator with semi natural commutation,” *2011 IEEE Energy Conversion Congress and Exposition*, Phoenix, AZ, USA, 2011, pp. 1119–1123.

[19] R. Echavarria, A. Claudio and M. Cotorogea, “Analysis, Design, and Implementation of a Fast On-Load Tap Changing Regulator,” in *IEEE Transactions on Power Electronics*, vol. 22, no. 2, pp. 527–534, March 2007.

[20] N. Burany, “Safe control of four-quadrant switches,” *Conference Record of the IEEE Industry Applications Society Annual Meeting,*, San Diego, CA, USA, 1989, pp. 1190–1194 vol.1.

[21] B. Park, S. Han and H. Cha, “Diode Bridge Embedded AlGaN/GaN Bidirectional Switch,” in *IEEE Electron Device Letters*, vol. 36, no. 4, pp. 324–326, April 2015.

[22] T. Morita *et al*., “650 V 3.1 mΩcm2 GaN-based monolithic bidirectional switch using normally-off gate injection transistor,” *2007 IEEE International Electron Devices Meeting*, Washington, DC, USA, 2007, pp. 865–868.

[23] Mansor, Muhamad & Abd Rahim, Nasrudin. (2012). “Three-Phase PWM-Switched Autotransformer Voltage-Sag Compensator Based on Phase Angle Analysis”, Arabian Journal for Science and Engineering, vol. 37, pp. 1–6, Nov. 2012.

[24] E. Afshari, M. Khodabandeh and M. Amirabadi, “A Single-Stage Capacitive AC-Link AC–AC Power Converter,” in *IEEE Transactions on Power Electronics*, vol. 34, no. 3, pp. 2104–2118, March 2019.

[25] I. Rankis and M. Prieditis, “Properties of the AC/AC buck-boost converter,” *2017 IEEE 58th International Scientific Conference on Power and Electrical Engineering of Riga Technical University (RTUCON)*, Riga, 2017, pp. 1–6.

[26] M. Prieditis and I. Rankis, “Necessity of low range voltage stabilization and solution with transformer based AC pulse modulation system,” *2015 IEEE 3rd Workshop on Advances in Information, Electronic and Electrical Engineering (AIEEE)*, Riga, Latvia, 2015, pp. 1–4.

[27] I. Rankis, M. Prieditis and D. Shirkin, “Transformer based AC pulse modulation system for voltage stabilization,” *2015 IEEE 5th International Conference on Power Engineering, Energy and Electrical Drives (POWERENG)*, Riga, Latvia, 2015, pp. 600–605.

[28] I. Rankis and M. Prieditis, “Buck mode control methods of the qZS-resonant DC/DC converters,” *2017 19th European Conference on Power Electronics and Applications (EPE'17 ECCE Europe)*, Warsaw, 2017, pp. P.1–P.16.

[29] J. Koscelnik, J. Sedo and B. Dobrucky, “Modeling of resonant converter with nonlinear inductance,” *2014 International Conference on Applied Electronics*, Pilsen, Czech Republic, 2014, pp. 153–156.

[30] Z. Fedyczak, L. Frackowiak, M. Jankowski and A. Kempski, “Single-phase serial AC voltage controller based on bipolar PWM AC matrix-reactance chopper,” *2005 European Conference on Power Electronics and Applications*, Dresden, Germany, 2005.

[31] G. Alain, R. Dominique and B. Hans-Peter, “AC line voltage controller for grid integration of renewable energy sources,” *2015 17th European Conference on Power Electronics and Applications (EPE'15 ECCE-Europe)*, Geneva, Switzerland, 2015, pp. 1–10.

[32] P. Li, D. Holliday and B. W. Williams, “AC voltage sag-swell compensator based on unified non-inverting and inverting output voltage ac chopper,” *8th IET International Conference on Power Electronics, Machines and Drives (PEMD 2016)*, Glasgow, UK, 2016, pp. 1–5.

[33] F. Hamoud, M. L. Doumbia and A. Chériti, “Voltage sag and swell mitigation using D-STATCOM in renewable energy based distributed generation systems,” *2017 Twelfth International Conference on Ecological Vehicles and Renewable Energies (EVER)*, Monte Carlo, Monaco, 2017, pp. 1–6.

[34] M. Nguyen, Y. Jung and Y. Lim, “Voltage swell/sag compensation with single-phase Z-source AC/AC converter,” *2009 13th European Conference on Power Electronics and Applications*, Barcelona, Spain, 2009, pp. 1–8.

[35] Q. Lei and F. Z. Peng, “Four quadrant voltage sag/swell compensation with interphase quasi-Z-source AC-AC topology,” *2011 Twenty-Sixth Annual IEEE Applied Power Electronics Conference and Exposition (APEC)*, Fort Worth, TX, USA, 2011, pp. 2013–2019.

[36] H. Elmasry, H. Z. Azazi, E. E. El-Kholy and S. A. Mahmoud, “Performance Analysis of Transformer-less Dynamic Voltage Restorer,” *2019 IEEE Conference on Power Electronics and Renewable Energy (CPERE)*, Aswan, Egypt, 2019, pp. 522–529.

[37] M. Nguyen, Y. Lim and J. Choi, “Single-phase Z-source-based voltage sag/swell compensator,” *2013 Twenty-Eighth Annual IEEE Applied Power Electronics Conference and Exposition (APEC)*, Long Beach, CA, USA, 2013, pp. 3138–3142.

[38] K. Yamamoto, S. Ehira and M. Ikeda, “Synchronous frame control for voltage sag/swell compensator utilizing single-phase matrix converter,” *2016 19th International Conference on Electrical Machines and Systems (ICEMS)*, Chiba, Japan, 2016, pp. 1–6.

[39] H. D. Vaidya *et al*., “Single-Phase Series Compensator Circuit for Mitigating Voltage Sag or Swell in the Power System Networks - Methodology and Modelling,” *2020 IEEE International Conference on Environment and Electrical Engineering and 2020 IEEE Industrial and Commercial Power Systems Europe (EEEIC / I&CPS Europe)*, Madrid, Spain, 2020, pp. 1–5.

[40] A. R. Gothane, B. B. Baliwant and V. B. Waghmare, “Simulation and Analysis of Series Active Filter Using AC-AC Converter for Mitigation of Sag,” *2019 3rd International Conference on Computing Methodologies and Communication (ICCMC)*, Erode, India, 2019, pp. 886–889.

[42] M. A. Santoyo Anaya, E. L. Moreno Goytia and J. R. Rodríguez, "The DVR-AC, a novel structure for mitigating large voltage sags and swells using voltage re-injection," *2011 North American Power Symposium*, Boston, MA, USA, 2011, pp. 1–6.

[43] B.N. Singh and M. Simina, "Intelligent solid-state voltage restorer for voltage swell/sag and harmonics", in *IEE Proceedings – Electric Power Applications*, 2004. pp. 98–106.

[44] B. KIM, S. AM, P. CHRIN, E. BOULAUD and E. BOISAUBERT, "Study of the Control of an AC Voltage Stabilizer Using LQR and Anti-windup," *2020 International Symposium on Power Electronics, Electrical Drives, Automation and Motion (SPEEDAM)*, Sorrento, Italy, 2020, pp. 623–627.

[45] J. V. Lopez, S. M. Garcia, J. C. C. Rodriguez, R. V. Garcia, S. M. Fernandez and C. C. Olay, "Electronic Tap-Changing Stabilizers for Medium-Voltage Lines Optimum Balanced Circuit," in *IEEE Transactions on Power Delivery*, vol. 27, no. 4, pp. 1909–1918, Oct. 2012.

[49] M. Farhoodnea, A. Mohamed and H. Shareef, "A comparative study on the performance of custom power devices for power quality improvement," *2014 IEEE Innovative Smart Grid Technologies - Asia (ISGT ASIA)*, Kuala Lumpur, Malaysia, 2014, pp. 153–157.

[50] M. Nguyen, Y. Jung and Y. Lim, "Voltage swell/sag compensation with single-phase Z-source AC/AC converter," *2009 13th European Conference on Power Electronics and Applications*, Barcelona, Spain, 2009, pp. 1–8.

[52] C. Ma, F. Gao, G. He and G. Li, "A Voltage Detection Method for the Voltage Ride-Through Operation of Renewable Energy Generation Systems Under Grid Voltage Distortion Conditions," in *IEEE Transactions on Sustainable Energy*, vol. 6, no. 3, pp. 1131–1139, July 2015.

[53] G. Lv and X. Wang, "Voltage Sags Detection and Identification Based on Phase-Shift and RBF Neural Network," *Fourth International Conference on Fuzzy Systems and Knowledge Discovery (FSKD 2007)*, Haikou, China, 2007, pp. 684–688.

[54] C. Fitzer, M. Barnes and P. Green, "Voltage sag detection technique for a dynamic voltage restorer," in *IEEE Transactions on Industry Applications*, vol. 40, no. 1, pp. 203–212, Jan.–Feb. 2004.

[55] S. Subramanian and M. K. Mishra, "Interphase AC–AC Topology for Voltage Sag Supporter," in *IEEE Transactions on Power Electronics*, vol. 25, no. 2, pp. 514–518, Feb. 2010.

[56] A. A. Khan, H. Cha and H. Kim, "Magnetic Integration of Discrete-Coupled Inductors in Single-Phase Direct PWM AC–AC Converters," in *IEEE Transactions on Power Electronics*, vol. 31, no. 3, pp. 2129–2138, March 2016.

[58] Z. Zhao, J. Yang, Q. Zhu, C. Wang and F. Jian, "A direct AC-AC converter for electronic power transformer based on energy injection control," *2016 2nd International Conference on Control Science and Systems Engineering (ICCSSE)*, Singapore, 2016, pp. 212–216.

[59] I. Rankis, M. Prieditis and D. Shirkin, "Transformer based AC pulse modulation system for voltage stabilization," *2015 IEEE 5th International Conference on Power*

Engineering, Energy and Electrical Drives (POWERENG), Riga, Latvia, 2015, pp. 600–605.

[61] I. Rankis, A. Vitols and M. Prieditis, “Investigation of the effectivness of nonlinear inductor in the AC/DC node of three phase rectifier,” *2019 IEEE 7th IEEE Workshop on Advances in Information, Electronic and Electrical Engineering (AIEEE)*, Liepaja, Latvia, 2019, pp. 1–7.

[62] Рожкова Л. Д., “Козулин В. С. Электрооборудование станций и подстанцийб” 1987. М: Энергоатомиздат, 648 стр.

[63] Ian Darney Updating Circuit Theory. The Voltage Injection Transformer, 2019, 8 pp.

[64] S. Sasitharan, M. K. Mishra, B. Kalyan Kumar and V. Jayashankar, “Rating and design issues of DVR injection transformer,” *2008 Twenty-Third Annual IEEE Applied Power Electronics Conference and Exposition*, Austin, TX, USA, 2008, pp. 449–455.

[65] Power Electronics handbook, editor in ch. Muhammad H. Rashid, Academic Press, New York, 2001, 895 pp.

[66] J. Kaniewski, Z. Fedyczak and P. Szczesniak, “AC voltage transforming circuits in power systems,” *2015 International School on Nonsinusoidal Currents and Compensation (ISNCC)*, Lagow, Poland, 2015, pp. 1–10.

[76] A. Khedekar, D. Badade, H. Ugawekar, S. Kale, R. D. Kulkarni and M. Kumari, “Simulation of Single Phase to Single Phase Step Down Cycloconverter for Industrial Application,” *2019 International Conference on Nascent Technologies in Engineering (ICNTE)*, Navi Mumbai, India, 2019, pp. 1–6.

[77] Vladimirs Cimanis, Vladimirs Hramcovs, Ivars Rankis, “Investigation of the Operation Speed of AC Voltage Sensor”, *Scientific Journal of Riga Technical University: Power and Electrical Engineering*, vol. 25, pp. 151–154, Jan. 2009.

.